Document made available under the Patent Cooperation Treaty (PCT)

International application number: PCT/JP04/019846

International filing date: 28 December 2004 (28.12.2004)

Document type: Certified copy of priority document

Document details: Country/Office: US
Number: 60/532,723
Filing date: 29 December 2003 (29.12.2003)

Date of receipt at the International Bureau: 17 March 2005 (17.03.2005)

Remark: Priority document submitted or transmitted to the International Bureau in compliance with Rule 17.1(a) or (b)

World Intellectual Property Organization (WIPO) - Geneva, Switzerland
Organisation Mondiale de la Propriété Intellectuelle (OMPI) - Genève, Suisse

PCT/JP2004/019846
25. 2. 2005

PA 1271864

THE UNITED STATES OF AMERICA

TO ALL TO WHOM THESE PRESENTS SHALL COME:

UNITED STATES DEPARTMENT OF COMMERCE

United States Patent and Trademark Office

January 13, 2005

THIS IS TO CERTIFY THAT ANNEXED HERETO IS A TRUE COPY FROM THE RECORDS OF THE UNITED STATES PATENT AND TRADEMARK OFFICE OF THOSE PAPERS OF THE BELOW IDENTIFIED PATENT APPLICATION THAT MET THE REQUIREMENTS TO BE GRANTED A FILING DATE UNDER 35 USC 111.

APPLICATION NUMBER: *60/532,723*
FILING DATE: *December 29, 2003*

By Authority of the
COMMISSIONER OF PATENTS AND TRADEMARKS

L. Edelen

L. EDELEN
Certifying Officer

15866 U.S.PTO

PTO/SB/16 (08-03)
Approved for use through 07/31/2006. OMB 0651-0032
U.S. Patent and Trademark Office; U.S. DEPARTMENT OF COMMERCE
Under the Paperwork Reduction Act of 1995, no persons are required to respond to a collection of information unless it displays a valid OMB control number

Provisional Application For Patent Cover Sheet

This is a request for filing a PROVISIONAL APPLICATION FOR PATENT under 37 C.F.R. 1.53(c).

Express Mail Label No.

INVENTOR(S)

Given Name (first and middle [if any])	Family Name or Surname	Residence (City and either State or Foreign Country)
Chikao Kei	Morimoto Ohnuma	Tokyo, Japan Tokyo, Japan

Additional inventors are being named on the ___ separately numbered sheets attached hereto.

22581 U.S.PTO 60/532723 12903

TITLE OF THE INVENTION (500 Characters Maximum)

Methods for Treating Diseases in Need of Regulation of Immune Response

CORRESPONDENCE ADDRESS

Direct all correspondence to:

☒ Customer number 26111

OR

☐ Firm *or* Individual Name	STERNE, KESSLER, GOLDSTEIN & FOX P.L.L.C.				
Address	1100 New York Avenue, N.W.				
Address					
City Washington		State	D.C.	ZIP	20005
Country	USA	Telephone	202-371-2600	Fax	202-371-2540

ENCLOSED APPLICATION PARTS (*check all that apply*)

☒ Specification *Number of pages* 33
☒ Drawing(s) *Number of sheets*: 14
☒ Application Data Sheet. See 37 CFR 1.76
☐ CD(s), Number ___
☒ Other (specify) Authorization Under 37 C.F.R. § 1.136(a)(3)

METHOD OF PAYMENT OF FILING FEES FOR THIS PROVISIONAL APPLICATION FOR PATENT (*check one*)

☐ Applicant claims small entity status. See 37 CFR 1.27.
☐ A check or money order is enclosed to cover the filing fees
☒ The Director is hereby authorized to charge filing fees or credit any overpayments to Deposit Account Number: 19-0036.
☒ Payment by credit card. Form PTO-2038 is attached.

Filing Fee Amount ($)160.00

The invention was made by an agency of the United States Government or under a contract with an agency of the United States Government.

☒ No

☐ Yes, the name of the U.S. Government agency and the Government contract number are:

Respectfully submitted,
Signature: Frank R. Cottingham
Typed or Printed Name: Frank R. Cottingham
Telephone: 202-371-2600

Date: DEC. 29, 2003
Registration No. 50,437 *(if appropriate)*
Docket Number: 2144.0150000/RWE/FRC

USE ONLY FOR FILING A PROVISIONAL APPLICATION FOR PATENT

This collection of information is required by 37 CFR 1.51. The information is required to obtain or retain a benefit by the public which is to file (and by the USPTO to process) an application. Confidentiality is governed by 35 U.S.C. 122 and 37 CFR 1.14. This collection is estimated to take 8 hours to complete, including gathering, preparing, and submitting the completed application form to the USPTO. Time will vary depending upon the individual case. Any comments on the amount of time you are required to complete this form and/or suggestions for reducing this burden, should be sent to the Chief Information Officer, U.S. Patent and Trademark Office, U.S. Department of Commerce, P.O. Box 1450, Alexandria, VA 22313-1450. DO NOT SEND FEES OR COMPLETED FORMS TO THIS ADDRESS. SEND TO: **Mail Stop Provisional Application, Commissioner for Patents, P.O. Box 1450, Alexandria, VA 22313-1450.**

If you need assistance in completing the form, call 1-800-PTO-9199 and select option 2.

PTO/SB/17 (08-03)
Approved for use through 07/31/2006. OMB 0651-0032
Patent and Trademark Office: U.S. DEPARTMENT OF COMMERCE
Under the Paperwork Reduction Act of 1995, no persons are required to respond to a collection of information unless it displays a valid OMB control number.

15886 U.S.PTO

FEE TRANSMITTAL for FY 2004

Effective 10/01/2003. Patent fees are subject to annual revision.

☐ Applicant claims small entity status. See 37 CFR 1.27

TOTAL AMOUNT OF PAYMENT ($)160.00

Complete if Known	
Application Number	T b assigned
Filing Date	D c mb r 29, 2003
First Named Inventor	Chikao M rimot
Examiner Name	N/A
Art Unit	N/A
Attorney Docket No.	2144.0150000/RWE/FRC

METHOD OF PAYMENT (check all that apply)

☐ Check ☒ Credit card ☐ Money Order ☒ Other** ☐ None

** Charge any deficiencies or credit any overpayments in the fees or fee calculations of Parts 1, 2 and 3 below to Deposit Account No. 19-0036.

☐ Deposit Account
Deposit Account Number 19-0036
Deposit Account Name: Sterne, Kessler, Goldstein & Fox P.L.L.C.

The Commissioner is authorized to: *(check all that apply)*

☒ Charge fee(s) indicated below ☒ Credit any over payments

☒ Charge any additional fee(s) during the pendency of this application

☐ Charge fee(s) indicated below, **except for the filing fee** to the above-identified deposit account.

FEE CALCULATION

1. BASIC FILING FEE

Large Entity Fee Code	Large Entity Fee ($)	Small Entity Fee Code	Small Entity Fee ($)	Fee Description	Fee Paid
1001	770	2001	385	Utility filing fee	
1002	340	2002	170	Design filing fee	
1003	530	2003	265	Plant filing fee	
1004	770	2004	385	Reissue filing fee	
1105	160	2005	80	Provisional filing fee	160.00

SUBTOTAL (1) ($) 160.00

2. EXTRA CLAIM FEES FOR UTILITY AND REISSUE

	Extra	Fee from below	Fee Paid
Total Claims ____ - 20** =	____	X ____	=
Indep. Claims ____ - 3** =	____	X ____	=
Multiple Dependent			=

Large Entity Fee Code	Large Entity Fee ($)	Small Entity Fee Code	Small Entity Fee ($)	Fee Description
1202	18	2202	9	Claims in excess of 20
1201	86	2201	43	Independent claims in excess of 3
1203	290	2203	145	Multiple dependent claim, if not paid
1204	86	2204	43	**Reissue independent claims over original patent
1205	18	2205	9	**Reissue claims in excess of 20 and over original patent

SUBTOTAL (2) ($)

***or number previously paid, if greater; For Reissue, see above*

FEE CALCULATION (continued)

3. ADDITIONAL FEES

Large Entity Fee Code	Large Entity Fee ($)	Small Entity Fee Code	Small Entity Fee ($)	Fee Description	Fee Paid
1051	130	2051	65	Surcharge - late filing fee or oath	
1502	50	2052	25	Surcharge-late provisional filing fee or cover sheet	
1053	130	1053	130	Non-English specification	
1812	2,520	1812	2,520	For filing a request for *ex parte* reexamination	
1804	920*	1804	920*	Requesting publication of SIR prior to Examiner action	
1805	1,840*	1805	1,840*	Requesting publication of SIR after Examiner action	
1251	110	2251	55	Extension for reply within first month	
1252	420	2252	210	Extension for reply within second month	
1253	950	2253	475	Extension for reply within third month	
1254	1,480	2254	740	Extension for reply within fourth month	
1255	2,010	2255	1,005	Extension for reply within fifth month	
1401	330	2401	165	Notice of Appeal	
1402	330	2402	165	Filing a brief in support of an appeal	
1403	290	2403	145	Request for oral hearing	
1451	1,510	1451	1,510	Petition to institute a public use proceeding	
1452	110	2452	55	Petition to revive - unavoidable	
1453	1,330	2453	665	Petition to revive - unintentional	
1501	1,330	2501	665	Utility issue fee (or reissue)	
1502	480	2502	240	Design issue fee	
1503	640	2503	320	Plant issue fee	
1460	130	1460	130	Petitions to the Commissioner	
1807	50	1807	50	Processing fee under 37 CFR 1.17(q)	
1806	180	1806	180	Submission of Information Disclosure Stmt	
8021	40	8021	40	Recording each patent assignment per property (times number of properties)	
1809	770	2809	385	Filing a submission after final rejection (37 CFR 1.129(a))	
1810	770	2810	385	For each additional invention to be examined (37 CFR 1.129(b))	
1801	770	2801	385	Request for Continued Examination (RCE)	
1802	900	1802	900	Request for expedited examination of a design application	

Other fee (specify) ____

* Reduced by Basic Filing Fee Paid SUBTOTAL (3) ($)

SUBMITTED BY				Complete *(if applicable)*	
Name (Print/Type)	Frank R. Cottingham	*Registration No. (Attorney/Agent)*	50,437	*Telephone*	202-371-2600
Signature	Frank R. Cottingham			*Date*	DEC. 29, 2003

WARNING: Information on this form may become public. Credit card information should not be included on this form. Provide credit card information and authorization on PTO-2038.

This collection of information is required by 37 CFR 1.17 and 1.27. The information is required to obtain or retain a benefit by the public which is to file (and by the USPTO to process) an application. Confidentiality is governed by 35 U.S.C. 122 and 37 CFR 1.14. This collection is estimated to take 12 minutes to complete, including gathering, preparing, and submitting the completed form to the USPTO. Time will vary depending upon the individual case. Any comments on the amount of time you require to complete this form and/or suggestions for reducing this burden, should be sent to the Chief Information Officer, U.S. Patent and Trademark Office, U.S. Department of Commerce, P.O. Box 1450, Alexandria, VA 22313-1450. DO NOT SEND FEES OR COMPLETED FORMS TO THIS ADDRESS. **SEND TO: Commissioner for Patents, P.O. Box 1450, Alexandria, VA 22313-1450.**

If you need assistance in completing the form, call 1-800-PTO-9199 (1-800-786-9199) and select option 2.

id: d b : USPTO from the IFW Image Database on 01/11/2005

Sterne Kessler Goldstein Fox
ATTORNEYS AT LAW

Robert Greene Sterne
Edward J. Kessler
Jorge A. Goldstein
David K.S. Cornwell
Robert W. Esmond
Tracy-Gene G. Durkin
Michele A. Cimbala
Michael B. Ray
Robert E. Sokohl
Eric K. Steffe
Michael Q. Lee
Steven R. Ludwig
John M. Covert
Linda E. Alcorn
Robert C. Millonig
Lawrence B. Bugaisky
Donald J. Featherstone
Michael V. Messinger

Judith U. Kim
Timothy J. Shea, Jr.
Patrick E. Garrett
Heidi L. Kraus
Edward W. Yee
Albert L. Ferro*
Donald R. Banowit
Peter A. Jackman
Molly A. McCall
Teresa U. Medler
Jeffrey S. Weaver
Kendrick P. Patterson
Vincent L. Capuano
Eldora Ellison Floyd
Thomas C. Fiala
Brian J. Del Buono
Virgil Lee Beaston
Kimberly N. Reddick

Theodore A. Wood
Elizabeth J. Haanes
Joseph S. Ostroff
Frank R. Cottingham
Christine M. Lhuller
Rae Lynn Prengaman
Jane Shershenovich*
Lawrence J. Carroll*
George S. Bardmesser
Daniel A. Klein*
Jason D. Eisenberg
Michael D. Specht
Andrea J. Kamage
Tracy L. Muller*
tuAnne M. Yuricek*
John J. Figueroa
Ann E. Summerfield
Tiera S. Coston*

Aric W. Ledford*

Registered Patent Agents•
Karen R. Markowicz
Nancy J. Leith
Helene C. Carlson
Gaby L. Longsworth
Matthew J. Dowd
Aaron L. Schwartz
Mary B. Tung
Katrina Y. Pei Quach
Bryan L. Skelton
Robert A. Schwartzman
Timothy A. Doyle
Jennifer R. Mahalingappa
Teresa A. Colella
Jeffrey S. Lundgren

Victoria S. Rutherford
Eric D. Hayes

Of Counsel
Kenneth C. Bass III
Evan R. Smith

*Admitted only in Maryland
*Admitted only in Virginia
•Practice Limited to Federal Agencies

U.S. PTO
122903

December 29, 2003

WRITER'S DIRECT NUMBER:
(202) 772-8615
INTERNET ADDRESS:
frankc@skgf.com

Commissioner for Patents
PO Box 1450
Alexandria, VA 22313-1450

Mail Stop Provisional Application

Re: U.S. Provisional Patent Application
Appl. No. To be assigned; Filed: December 29, 2003
For: **Methods for Treating Diseases in Need of Regulation of Immune Response**
Inventors: Morimoto *et al.*
Our Ref: 2144.0150000/RWE/FRC

Sir:

The following documents are being submitted under 37 C.F.R. § 1.53(c) herewith for appropriate action by the U.S. Patent and Trademark Office:

1. PTO Fee Transmittal (Form PTO/SB/17);

2. Authorization to Treat a Reply As Incorporating An Extension of Time Under 37 C.F.R. § 1.136(a)(3);

3. Application Data Sheet (37 C.F.R. § 1.76);

4. A Provisional Application for Patent Cover Sheet;

5. U.S. Provisional Patent Application entitled:

Methods for Treating Diseases in Need of Regulation of Immune Response

and naming as inventors: **Chikao Morimoto**
Kei Ohnuma

the application consisting of:

a. A specification containing 33 total pages:

(i) 31 pages of description prior to any claims; and

(ii) 2 pages of claims (14 claims);

b. 14 sheets of drawings: (Figs.: 1A-1C, 1D-1E, 1F-1G, 1H, 2A-2C, 2D, 3A-3C, 3D-3G, 4A-4B, 4C-4D, 5A-5C, 5D, 6A, and 6B);

6. Form PTO-2038 Credit Card Payment Form in the amount of **$160.00** to cover the filing fee; and

7. Two (2) return postcards.

It is respectfully requested that, of the two attached postcards, one be stamped with the filing date of these documents and returned to our courier, and the other, prepaid postcard, be stamped with the filing date and returned as soon as possible.

The U.S. Patent and Trademark Office is hereby authorized to charge any fee deficiency, or credit any overpayment, to our Deposit Account No. 19-0036.

Respectfully submitted,

STERNE, KESSLER, GOLDSTEIN & FOX P.L.L.C.

Frank R. Cottingham

Frank R. Cottingham
Attorney for Applicants
Registration No. 50,437

FRC/pcd
Encls.

SKGF_DC1:213678.1

Copy provided by USPTO from the IFW Image Database on 01/11/2005

IN THE UNITED STATES PATENT AND TRADEMARK OFFICE

In re application of:	Confirmation No. To be assigned
Morimoto *et al.*	Art Unit: N/A
Appl. No. To be assigned	Examiner: N/A
Filed: December 29, 2003	Atty. Docket: 2144.0150000/RWE/FRC
For: **Methods for Treating Diseases in Need of Regulation of Immune Response**	

Authorization To Treat A Reply As Incorporating An Extension Of Time Under 37 C.F.R. § 1.136(a)(3)

Commissioner for Patents
PO Box 1450
Alexandria, VA 22313-1450

Sir:

The U.S. Patent and Trademark Office is hereby authorized to treat any concurrent or future reply that requires a petition for an extension of time under this paragraph for its timely submission, as incorporating a petition for extension of time for the appropriate length of time. The U.S. Patent and Trademark Office is hereby authorized to charge all required extension of time fees to our Deposit Account No. 19-0036, if such fees are not otherwise provided for in such reply.

Respectfully submitted,

STERNE, KESSLER, GOLDSTEIN & FOX P.L.L.C.

Frank R. Cottingham
Attorney for Applicants
Registration No. 50,437

Date: DEC. 29, 2003

1100 New York Avenue, N.W.
Washington, D.C. 20005-3934
(202) 371-2600

::ODMA\MHODMA\SKGF_DC1;213667;1

Copy provided by USPTO from the IFW Image Database on 01/11/2005

Methods for Treating Diseases in Need of Regulation of Immune Response

Summary

CD26 is a T cell costimulatory molecule with dipeptidyl peptidase IV (DPPIV) activity in its extracellular region. We previously reported that recombinant soluble CD26 (rsCD26) enhanced peripheral blood T cell proliferation induced by the recall antigen tetanus toxoid (TT). However, the mechanism involved in this immune enhancement is not yet elucidated. We now demonstrated that CD26 bound Caveolin-1 on APC, and identified that residues 201 to 211 of CD26 along with the serine catalytic site at residue 630, which constitute a pocket structure of CD26 / DPPIV, contributed to binding to caveolin-1 scaffolding domain. In addition, following CD26-caveolin-1 interaction on TT-loaded monocytes, caveolin-1 was phosphorylated and released Tollip from caveolin-1 into the cytoplasm. Release of Tollip from caveolin-1 was associated with phosphorylation of IRAK, which links to activated NF-κB, followed by upregulation of CD86. Finally, inhibition of caveolin-1 expression on monocytes resulted in lack of CD86 upregulation by CD26. Taken together, these results suggested that CD26-caveolin-1 interaction plays a role in the upregulation of CD86 on TT-loaded monocytes and subsequent engagement with CD28 on T cells, leading to antigen-specific T cell activation.

Copy provided by USPTO from the IFW Image Database on 01/11/2005

Introduction

CD26 is a widely distributed 110-kDa cell surface glycoprotein with known dipeptidyl peptidase IV (DPPIV, EC3.4.14.5) activity in its extracellular domain (Morimoto, et al., 1998; von Bonin et al., 1998). This enzyme is capable of cleaving amino-terminal dipeptides with either L-proline or L-alanine at the penultimate position. The expression of CD26 is enhanced after activation of T cells in a resting state. In addition, the CD4+CD26^{high} T cells respond maximally to recall antigens such as tetanus toxoid (Morimoto, et al., 1989). Accumulating evidence suggests that DPPIV enzyme activity plays a role in the immune response (Oravecz et al., 1997; Iwata, et al., 1999). Crosslinking of CD26 and CD3 with solid-phase immobilized monoclonal antibodies (mAbs) can induce T cell costimulation and IL-2 production by either human CD4+ T cells or Jurkat T cell lines transfected with CD26 cDNA (Tanaka, et al., 1992; Fleischer, et al., 1994). In addition, anti-CD26 antibody treatment of T cells leads to a decrease in the surface expression of CD26 via its internalization, and such modulation results in an enhanced proliferative response to anti-CD3 or anti-CD2 stimulation as well as enhanced tyrosine phosphorylation of signaling molecules such as CD3ζ and p56-Lck (Hegen, et al., 1997). Moreover, we showed that DPPIV enzyme activity is required for the CD26-mediated T cell costimulation (Tanaka, et al., 1993). More recently, we have shown that internalization of CD26 after crosslinking is mediated in part by the mannose-6-phosphate/insulin-like growth factor II receptor (M6P/IGF-IIR), and that the interaction of CD26 and M6P/IGFIIR plays a role in CD26-induced T cell costimulation (Ikushima, et al., 2000).

Maximal T cell activation requires both an antigen (Ag)-specific stimulus provided by an MHC peptide complex and a costimulatory signal (Lenschow, et al., 1996). Engagement of CD28 on the surface of T cells by B7-1 (CD80) or B7-2 (CD86) expressed on antigen presenting cells (APC) provides a potent costimulatory signal (Yokochi, et al., 1982; Azuma, et al., 1993; Freeman, et al., 1993; Lenschow, et al., 1996; McAdam, et al., 1998). CD28-B7 interactions lead to T cell proliferation, differentiation, and cytokine secretion (McAdam, et al., 1998; Chambers, 2001). In contrast, engagement of CTLA-4 on activated T cells by B7-1 or B7-2 results in an inhibition of T cell responses (Croft, et al., 1992; Walunas, et al., 1994; Krummel, et al., 1995). However, only CD28 is constitutively expressed, and hence it has an important role in the generation of T cell immune response (Fraser, et al., 1992; Caux, et al., 1994; Hathcock, et al., 1994; Yi-qun, et al., 1996; Hakamada-Taguchi, et al., 1998; Manickasingham, et al., 1998).

In our previous report, we have shown that recombinant soluble CD26 (rsCD26) enhanced proliferative responses of peripheral blood lymphocytes (PBLs) to stimulation with the soluble antigen tetanus toxoid (TT) (Tanaka, et al., 1994). More recently, we demonstrated

Copy provided by USPTO from the IFW Image Database on 01/11/2005

that the target cells of rsCD26 were the CD14 positive monocytes in the peripheral blood, and that rsCD26 could upregulate CD86 expression, but not CD80 or HLA-DR antigen levels on monocytes (Ohnuma, et al., 2001). M6P/IGF-IIR is thought to be one of the platform molecules for CD26 interaction with APC. However, while both DPPIV-positive and DPPIV-negative rsCD26 were taken up by monocytes via M6P/IGF-IIR, only DPPIV-positive rsCD26 displayed an effect of CD86 upregulation on monocytes, thus suggesting that additional factors may interact with CD26 to directly induce CD86 upregulation on monocytes. Moreover, the molecular mechanism for the maximal response of CD4+CD26^{high} T cells to the memory antigens has not yet been clarified.

In the present study, we attempted to identify CD26-interacting molecules directly involved in the upregulation of CD86. We demonstrated that CD26 bound caveolin-1 on APC, and identified that residues 201 to 211 in CD26 along with the serine catalytic site at residue 630, which constitute a pocket structure of CD26 / DPPIV (Rasmussen, et al., 2003), contributed to binding to the scaffolding domain of caveolin-1. Following binding of CD26 to caveolin-1 on APC, caveolin-1 was phosphorylated and released Tollip (Toll-interacting protein) from caveolin-1 into the cytosole. Moreover, release of Tollip from caveolin-1 led to phosphorylation of IRAK (interleukin-1 receptor (IL-1R) associated serine / threonine kinase), which links to activated NF-κB, followed by upregulation of CD86 and subsequent engagement of CD28 molecule on T cells.

Copy provided by USPTO from the IFW Image Database on 01/11/2005

RESULTS

Identification of CD26 binding protein

To identify CD26-interacting proteins in monocytes, we generated CD26-bound affinity columns with ADA-sepharose, since ADA is a CD26-binding protein (Kameoka, et al., 1993). Cellular extracts from the monocyte cell line THP-1 were applied to this CD26-ADA sepharose column. After vigorous washing, bound proteins were eluted using highly concentrated salt buffer. These proteins were then subjected to SDS-PAGE analysis. Non-specific multiple bands were found in lanes of lysate, elution of ADA (mock) column, and washout solution after eluting through CD26-ADA columns (lanes 1-3 in Figure 1A). On the other hand, three major bands were revealed in the elution of CD26-ADA columns (lane 4 in Figure 1A). The protein bands specifically bound to CD26 on ADA columns were subjected to peptide mass fingerprinting by matrix assisted laser desorption ionization time-of-flight mass spectrometry (MALDI-TOF MS). With searching of the MASCOT database, obtained masses and apparent molecular weights of the different polypeptides revealed that the fraction eluted from CD26-ADA sepharose columns contained three major bands, and these bands were determined to be CD26, ADA and Caveolin-1 (Figure 1A). Since CD26-ADA beads were generated with passive conjugation, CD26 and ADA in the elution fraction might be contaminated from column beads. Caveolin-1 at approximately 20-25 kDa was strongly stained with silver in the elution fraction (lane 4), and was not detected specifically in the fraction through the mock ADA beads column (lane 2). These findings suggested that caveolin-1 was associated with the CD26 molecule.

To confirm the interaction between CD26 and caveolin-1 in living cells, we next performed coimmunoprecipitation experiments. After the addition of rsCD26-wt to THP-1 cells, CD26 was detected by its specific antibody in lysates coimmunoprecipitated with caveolin-1 specific antibody (left panel of Figure 1B). Endogenous caveolin-1 was detected in THP-1 (lower of left panel in Figure 1B). Caveolin-1 was detected specifically with Western blots of lysates coimmunoprecipitated with CD26 specific antibody (upper of right panel in Figure 1B). Endogenous CD26 was not detected in THP-1 (lower of right panel in Figure 1B). Thus, the above results showed that caveolin-1 is the binding protein to CD26 in THP-1.

To determine the binding domain of caveolin-1 to CD26, we performed a GST pull-down assay using a series of GST-fused deletion mutants of caveolin-1 (Figure 1C), and CD26 transfected Jurkat T cells (J.CD26). As shown in Figure 1D, CD26 was co-precipitated with GST-Cav-1 wt, Cav-1 (1-101), and Cav-1 (82-178), but not with GST-Cav-1 (1-82), Cav-1 (102-178) and Cav-1 (del82-101), indicating that residues 82-101 of caveolin-1 is the binding domain to CD26. This domain is known as the scaffolding domain (SCD) of caveolin-1 (Smart,

Copy provided by USPTO from the IFW Image Database on 01/11/2005

et al., 1999). To confirm these findings in living cells, we constructed GFP-fused full-length caveolin-1 and caveolin-1 lacking the scaffolding domain (del 82-101). After the GFP-fused caveolin-1 and its mutant were transfected into HEK293 cells, which did not express either CD26 nor caveolin-1, Texas red conjugated CD26 (sCD26-TR) was added to the transfectants. Full-length caveolin-1-GFP, which was detected in surface membrane and perinuclear area (Figure 1E-a), was clearly merged with sCD26-TR (Figure 1E-b, c). On the other hand, since caveolin residues 61-101 was demonstrated to be necessary for oligomerization (Smart, et al., 1999), caveolin (del 82-101)-GFP lacking its scaffolding domain was localized diffusely (Figure 1E-d), and showed no evidence of interacting with sCD26-TR (Figure 1E-e, f). Although CD26-TR was slightly detected in HEK293 cells transfected with GFP alone (Figure 1E-g, h), CD26-TR was not associated with GFP (Figure 1E-i).

To determine the region(s) in CD26 responsible for binding to caveolin-1, we next performed a GST-pull down assay using a series of GST-fused deletion mutants of CD26 produced by COS-7 cells (Figure 1F). To preserve the natural composition of CD26, we constructed a series of GST-fused deletion mutants of CD26 expressed in COS cells, using GST-fused proteins vector expressed in mammalian cells (Sanchez, et al., 1994). As shown in Figure 1G, caveolin-1 was co-precipitated with GST-CD26 wt, and CD26 D3 (residues 31-429), but did not coprecipitate with GST-CD26 D1 (residues 507-766), CD26 D2 (residues 267-584), and CD26 del 201-211. These results suggested that amino acids 201-211 of CD26 were required for binding of CD26 to caveolin-1. This region in CD26 contains a caveolin-binding consensus motif (CBD) ($\phi X\phi XXXX\phi XX\phi$; ϕ and X depict aromatic residue and any amino acid, respectively) (Smart, et al., 1999), specifically WVYEEEVFSAY (Tanaka, et al., 1992). Our previous report revealed that DPPIV enzymatic activity of CD26 was necessary to exert activation effect of TT-loaded monocytes (Ohnuma, et al., 2001). In this regard, caveolin-1 was not detected in complexes with GST-CD26 S630A, with DPPIV enzymatic activity being deleted (Figure 1G). To confirm these findings in living cells, we constructed GFP-fused full-length CD26, mutant lacking CBD (del 201-211) and mutant lacking DPPIV enzymatic activity (S630A). After the GFP-fused CD26 and mutants were transfected into HEK293 cells, Texas red conjugated caveolin-1 (cav-TR) was added to the transfectants. CD26 wt-GFP, CD26 del201-211-GFP and CD26 S630A-GFP were localized in cell surface membrane (Figures 1H-a, d, g). Cav-TR was colocalized in HEK293 cells transfected with CD26-wt-GFP (Figures 1H-b, c). In CD26 (del201-211) as well as CD26 S630A-GFP transfected cells, however, cav-TR was not detected (Figures 1H-e, f, h, i). Cav-TR was not observed in HEK293 cells transfected with GFP alone (Figures 1H-j, k, l). To confirm the role of DPPIV active site in binding of CD26 to caveolin-1, we used the competitive inhibitor of DPPIV, valine-pyrrolidide (Val-Pyr). After GFP-CD26 wt transfected HEK293 cells were treated with

Copy provided by USPTO from the IFW Image Database on 01/11/2005

Val-Pyr (Figure 1H-m), cav-TR was added to the cells. Cav-TR was not observed in HEK293 cells transfected with GFP-CD26 wt after treatment with Val-Pyr (Figures 1H-n, o). Since the binding of Texas red conjugated-ADA to CD26 was observed in HEK293 cells transfected with GFP-CD26 wt after treatment with Val-Pyr (Figures 1H-p, q, r), Val-Pyr did not change the nature of the transfectants as well as the binding activity of CD26. Taken together, CD26 is demonstrated to bind to caveolin-1 through CBD as well as the serine residue 630 in CD26 and the scaffolding domain in caveolin-1.

CD26 on T cells interacts with caveolin-1 on monocytes

Caveolin-1 was demonstrated to be localized to the cytoplasmic membrane inner layer, toward the cytosolic side (Smart, et al., 1999). Our previous data showed that rsCD26 upregulated CD86 on monocytes only after treatment with the recall antigen tetanus toxoid (TT) (Ohnuma, et al., 2001). Since TT was reported to be taken up by antigen presenting cells (APC) through caveolae (Montesano, et al., 1982; Pelkmans, et al., 2002), we next examined a flip-flop event of caveolin-1 in monocytes after treatment with TT. To detect caveolin-1, we used anti-caveolin-1 polyclonal antibody detecting the N terminus of caveolin-1. In the presence or absence of TT treatment of purified monocytes, we evaluated for potential caveolin-1 presence on the cell surface. Using FCM, caveolin-1 was detected on cell surface of monocytes 12-24 hours after treatment with TT (Figure 2A). On the other hand, caveolin-1 on untreated monocytes was not detected after 0-48 hours of culture. To further examine TT effect on caveolae, we used monocytes treated with Filipin, which inhibits caveolae trafficking by dispersing cholesterol in cell membrane (Peiro, et al., 2000). As shown in Figure 2A, caveolin-1 was not detected on monocytes treated with Filipin, even after TT was loaded. These data demonstrated that certain populations of TT-loaded monocytes were found to express caveolin-1 on cell surface.

Since $CD26^{high}$ T cells strongly responded to memory antigens such as TT (Morimoto, et al., 1989), and activated $CD26^{high}$ T cells are accumulated in the inflammatory regions (Morimoto, et al., 1998; von Bonin, et al., 1998), we hypothesized that activated memory T cell – antigen-loaded monocytes interacted directly via surface expressed CD26 on T cells and caveolin-1 on monocytes. To further characterize these points, we examined potential colocalization of CD26 and caveolin-1 in T cell-monocyte contact site. For this purpose, activated peripheral T cells were mixed with TT-loaded monocytes, and conjugate formation was then initiated by centrifuging these cell mixtures. 30 minutes later, cells were prepared for confocal laser microscopy as described in Experimental Procedures. As reported previously, T cells did not express caveolin-1 (Galbiati, et al., 2001) and resting monocytes did not express CD26 (Morimoto, et al., 1989) as shown in Figures 2B-a, b, and c. On the other hand, CD26

Generated by USPTO from the IFW Image Database on 01/11/2005

and caveolin-1 were recruited in the contact area of activated T cells and TT-loaded monocytes (Figure 2C-a to i). Quantification of cell conjugation between T cells and monocytes was shown in Figure 2D. As shown in caveolin-1 expression study (Figure 2A), conjugation formation of activated T cells and TT-loaded monocytes was increased in monocytes with TT loaded for 12-24 hrs (solid circle in Figure 2D). Cell conjugation was not detected in TT-untreated monocytes or with Filipin-treated monocytes(open circle, solid triangle, and open triangle in Figure 2D). These data suggested that memory CD26+ T cells interacted with antigen-loaded monocytes through interaction of CD26 on T cells and caveolin-1 expressed on monocytes.

Phosphorylation of caveolin-1 leads to signal transduction in monocytes

We next focused on caveolin-1-mediated signal transduction events and determined whether such events upregulate CD86 expression following CD26 binding to caveolin-1 on TT-loaded monocytes. To stimulate TT-loaded monocytes with CD26, we used CD26 coated polystyrene latex beads to mimic the physiological interaction of CD26 expressed on peripheral T cells and TT-loaded monocytes. Figure 3A-a shows that beads coated with wild type CD26 engaged caveolin-1 on TT-loaded monocytes, whereas beads coated with mutant CD26 lacking CBD did not alter caveolin-1 expression on TT-loaded monocytes (Figure 3A-b). It is reported that in signaling events via caveolin-1, phosphorylation of caveolin-1 was implicated (Smart, et al., 1999). For this purpose, at various time periods following stimulation of TT-loaded monocytes by these beads, cell lysates were prepared for analysis. 0.5-10 minutes following stimulation with CD26 wt-coated beads, caveolin-1 was phosphorylated (Figure 3B), and the changes in intensity were shown as a bar graph in the bottom panel of Figure 3B. The signaling cascade leading to CD86 upregulation appears to involve a number of proteins, such as MyD88, IRAK, and Tollip (Medzhitov, 2001). MyD88 and IRAK contain the Toll-IL-1-receptor domain and the death domain for interacting with each other or the IL-1 receptor or Toll-like receptor (Medzhitov, 2001). Tollip contains a C2 domain (Protein kinase C conserved region 2), which was predicted, but not yet clearly demonstrated, to be associated with membrane lipids (Burns, et al., 2000). The C2 domain is a region containing approximately 130 residues involved in binding phospholipids in a calcium dependent manner or calcium independent manner. C2 domains are found in over 100 different proteins with functions ranging from signal transduction to vesicular trafficking. Calcium binding to the C2 domain of synaptotagmin induces little conformational change in the C2 domain, but calcium induces a change in the electrostatic potential to enhance phospholipid binding, suggesting the C2 domain functions as an electrostatic switch. In addition to electrostatic interactions, side chains in the calcium binding loops influence the binding of different C2 domains to either neutral or

Copy provided by USPTO from the IFW Image Database on 01/11/2005

negatively charged phospholipids. Tollip C2 domain was not reported to be associated with calcium dependent action in the IL-1 receptor or Toll-like receptor signaling (Medzhitov, 2001). We therefore examined the potential involvement of these proteins in signaling cascade via CD26-caveolin-1 interaction. As shown in Figure 3B, Tollip was found in IP complexes with caveolin-1 pAb, and released from caveolin-1 2-5 minutes after CD26-caveolin-1 interaction (between 2 to 5 min, Tollip was not detected in IP complex with caveolin-1 pAb). At these time points, IRAK showed hyperphosphorylation (Figure 3B) by Western blot analysis. It should be noted that neither MyD88 nor IRAK-4 was observed in the complexes (data not shown). On the other hand, caveolin-1 was not phosphorylated after stimulation with mutant CD26 (del201-211) beads, nor release of Tollip, nor shift of IRAK (Figure 3C). These results suggested that the Tollip-IRAK cascade was triggered by CD26-caveolin-1 interaction.

Previous reports demonstrated that Tollip was present in a complex with IRAK, and that recruitment of Tollip-IRAK complexes to the activated IL-1 receptor or Toll-like receptor complexes led to activation of NF-κB (Cao, et al., 1996; Burns, et al., 2000). The above results suggested that Tollip in monocytes was present in a complex with caveolin-1. We next examined in detail the association between caveolin-1 and Tollip. IP study in monocytes shown in Figures 3B and C revealed that caveolin-1 was associated with Tollip. In living cells, Tollip was partially colocalized with caveolin-1 in THP-1 cells transfected with GFP-fused caveolin-1, especially in surface membrane (Figures 3D-a, b, and c). To further determine the binding domains of Tollip-caveolin-1 complexes, we performed a GST-pulldown assay using a series of GST-fused caveolin-1 and GST-fused Tollip mutants (Figures 1C and 3F). As shown in Figures 3E, Tollip was coprecipitated with GST-Cav-1 wt, Cav-1 (1-101), and Cav-1 (82-178), implying that the scaffolding domain of caveolin-1 (residues 82-101) was required for binding to Tollip. As shown in Figures 3G, caveolin-1 was coprecipitated with GST-Tollip wt, Tollip (47-274), Tollip (1-178), and Tollip (47-178). These results revealed that the C2 domain of Tollip (residues 47-178) was associated with caveolin-1 interaction. Taken together, after ligation of caveolin-1 on TT-loaded monocytes by binding of CD26, caveolin-1 was phosphorylated and released Tollip, associated with phosphorylation of IRAK in monocytes.

NF-κB activation is required for CD86 upregulation after CD26-caveolin-1 interaction

Our data above suggested that IRAK might play a role in CD86 upregulation in monocytes as a downstream event of CD26-caveolin-1 interaction. Previous studies reported that IRAK phosphorylation was associated with TRAF6 to induce activation of NF-κB, JNK (c-Jun N-terminal kinase) and p38 MAP kinase (Cao, et al., 1996). We next identified the transcriptional factors activated by CD26 in the presence of TT-loaded monocytes. Using ELISA-based DNA-binding detection method, we detected significant levels of p50 and p65

Copy provided by USPTO from the IFW Image Database on 01/11/2005

NF-κB components in nuclear extracts of TT-loaded monocytes stimulated with wild type CD26 (right panel of Figure 4A). The increase in p50 and p65 NF-κB levels was inhibited by the specific competitor oligos (left panel of Figure 4A). Levels of AP-1 (c-Fos and c-Jun) and STAT1 were not detected in nuclear extracts of TT-loaded monocytes stimulated with wild type CD26 (Figure 4A). These results suggested that NF-κB was activated via IRAK phosphorylation after Tollip was released from caveolin-1. We next examined whether NF-κB binding sites were required in the human CD86 promoter regions for activation, since previous reports revealed that GAS elements (gamma-interferon activation sites) and NF-κB binding sites were present and required for activation of CD86 transcription (Li, et al., 1999). For this purpose, we constructed a series of luciferase chimera mutants of 5'-flanking promoter region of human CD86 (Figure 4B). Using these luciferase mutants, we tested CD86 promoter activity after CD26-caveolin-1 interaction. In the presence or absence of GAS elements (pGL3-Luc/1181 and pGL3-Luc/783), luciferase activity was not affected following stimulation of TT-loaded monocytes with CD26 (Figures 4C). On the other hand, two NF-κB binding sites in the promoter regions were required for activation of CD86 transcription following CD26 treatment in caveolin-1 expressed HEK293 cells (Figure 4C). In contrast, significant activity in single NF-κB luciferase construct (pGL3-Luc/409) was not detected (Figure 4C). It should be noted that no significant activity in NF-κB luciferase was observed in cells treated with rsCD26 or cells with caveolin-1 alone. Moreover, an enhancement in luciferase activity was observed with increasing doses of rsCD26 wt in HEK293 cells transfected with pGL3-Luc/1181 and caveolin-1 (Figure 4D). This dose dependent luciferase activity was not observed following stimulation with CD26 del201-211. These results showed that NF-κB activation downstream of cavelin-1 resulted in the upregulation of CD86 in TT-loaded monocytes stimulated with CD26.

siRNA against caveolin-1 in monocytes attenuates upregulation of CD86 by CD26 treatment

To examine CD26-caveolin-1 interaction and its functional consequences more directly, we performed siRNA experiments utilizing freshly isolated monocytes. We first tested whether siRNA was successfully transfected into primary monocytes. For this purpose Texas red conjugated siRNA (siRNA-TR) was used and visualized by confocal laser microscopy. As shown in Figure 5A, more than 95% of monocytes were transfected with siRNA-TR, using HVJ-E (Hemagglutinating Virus of Japan Envelope) vector and centrifugation method. We next examined by Western blot analysis whether siRNA against caveolin-1 was effective in knocking down caveolin-1 protein levels in transfected monocytes. We prepared 2 sets of specific siRNA against caveolin-1 as described in Experimental Procedures, and both of these

Copy provided by USPTO from the IFW Image Database on 01/11/2005

siRNA effectively knocked down caveolin-1 expression in monocytes (Figure 5B). Since caveolin-1 in monocytes was not significantly knocked down by mismatched siRNA or HVJ-E vector alone, this inhibitory effect by siRNA was specific. We next examined whether CD26 exerted its effect in monocytes in which caveolin-1 expression was knocked down by siRNA. CD86 was upregulated among a significant population of TT-loaded monocytes stimulated with CD26 wt-coated beads (right of upper panels in Figure 5C). On the other hand, sense siRNA (ss1 and ss2) inhibited this effect on CD86 upregulation in TT-loaded monocytes (middle and right of lower panels in Figure 5C). Mismatched siRNA did not exhibit this inhibitory effect (left of lower panel in Figure 5C). Changes in CD86 expression were clearly demonstrated in Figure 5D, demonstrating that knockdown of the caveolin-1 expression resulted in the inhibition of CD86 upregulation in TT-loaded monocytes stimulated with CD26 (* and ** in Figure 5D). These results suggested that caveolin-1 played an important role in signal transduction following CD26 binding to TT-loaded monocytes, leading to the upregulation of CD86 in monocytes.

Copy provided by USPTO from the IFW Image Database on 01/11/2005

Discussion

In the present study, to identify candidate binding proteins to CD26, we attempted to isolate the candidate proteins using a biochemical approach based on the THP-1 monocyte cell line, demonstrating that caveolin-1 was the binding protein. We showed that CD26 on activated memory T cells interacted with caveolin-1 on tetanus toxoid (TT) -loaded monocytes. In this interaction, caveolin-1 residues 82-101, the scaffolding domain, was associated with CD26 residues 201-211, the caveolin binding motif.

In the process of T cell proliferative response against a recall antigen, several major factors have been shown to contribute to the maintenance of the biological reaction, including APC, helper T cells, and selected cytokines (Yokochi, et al., 1982; Azuma, et al., 1993; Freeman, et al., 1993; Lenschow, et al., 1996; Hathcock, et al., 1994; Yi-qun, et al., 1996; McAdam, et al., 1998; Hakamada-Taguchi, et al., 1998; Manickasingham, et al., 1998; Chambers, 2001). Initially, an APC-T cell interaction plays a key role in triggering the T cell response, leading eventually to the expression of the T cell biological program (Lenschow, et al., 1996; McAdam, et al., 1998; Chambers, 2001). Our previous studies showed that the enhancing effect of rsCD26 on TT-induced T cell proliferation occurred in the early stages of the immune response (Ohnuma, et al., 2001). Moreover, we demonstrated that the target cells of rsCD26 were the CD14 positive monocytes in the peripheral blood, and that rsCD26 could upregulate CD86 expression, but not CD80 or HLA-DR antigen levels on monocytes (Ohnuma, et al., 2001). M6P/IGF-IIR is thought to be one of the platform molecules for CD26 interaction with APC. However, both DPPIV-positive and DPPIV-negative rsCD26 were taken up by monocytes via M6P / IGF-IIR, but only uptake of DPPIV-positive rsCD26 resulted in CD86 upregulation on monocytes. Furthermore, rsCD26 was taken up by 293 cells without caveolin-1 (Figure 1D) as well as by resting monocytes (Ohnuma, et al., 2001). M6P / IGF-IIR may have a role in rsCD26-monocyte interaction for other functions such as scavenging. Therefore, additional molecules may interact with CD26, leading to CD86 upregulation. Moreover, in-depth mechanism for the preferential response of $CD26^{high}$ T cells to the memory antigen and precise signaling events in CD86 upregulation on monocytes by rsCD26 remain to be elucidated. While it has been reported that the 300 kDa protein M6P / IGF-IIR was linked with CD26 on T cell surface to enhance CD26-mediated costimulation (Ikushima, et al., 2000), no protein of molecular weight of approximately 300 kDa was detected by our present purification method. An explanation may be that M6P / IGF-IIR might compete with ADA to bind CD26 since we used CD26-ADA sepharose bead columns to purify potential CD26-associated molecules. Alternatively, our detection approach may miss this protein due to the relatively high molecular weight of 300 kDa of M6P/IGF-IIR.

Caveolin-1 is the primary coat protein of caveolae, and is involved as a regulator of

Copy provided by USPTO from the IFW Image Database on 01/11/2005

signal transduction through binding of its scaffolding domain to key signaling molecules in various cells (Smart, et al., 1999; Peiro, et al., 2000; Carver, et al., 2003). Although CD26 was present in caveolae of fibroblast-like synoviocytes (Riemann, et al., 2001), its direct binding or signaling event was not demonstrated in immune cells. We showed here that CD26 was directly bound to caveolin-1 using a series of CD26 and caveolin-1 deletion mutants, and that caveolin-1 was phosphorylated following binding to CD26. Caveolin-1 was reported to be an integral membrane protein with a cytoplasmic N-terminal domain and a cytoplasmic C-terminal domain (Smart, et al., 1999). Our present data showed that the N-terminal domain of caveolin-1 was expressed on cell surface of monocytes 12-24 hrs after tetanus toxoid was loaded (Figure 2A). Since tetanus toxoid was trafficked in cells through caveolae (Montesano, et al., 1982; Pelkmans, et al., 2002), caveolin-1 may be transported with the peptide-MHC complex developed in APC, and be expressed on cell surface by antigen-processing machinery for T cell contact (Grakoui, et al., 1999; Turley, et al., 2000). Our data shown in Figure 2C indicated that CD26 on activated memory T cells directly faced caveolin-1 on TT-loaded monocytes in the contact area, which was revealed as the immunological synapse for T cell-APC interaction. It is conceivable that the interaction of CD26 with caveolin-1 on antigen-loaded monocytes resulted in the upregulation of CD86, therefore enhancing the subsequent interaction of CD86 and CD28 on T cells to induce antigen-specific T cell proliferation and activation.

By studying the crystal structure of CD26/DPPIV, the horizontal helix of residues 201-207 was situated in front of the DPPIV enzyme active site at the serine residue 630. This small horizontal cavity allowed substrate amino acids to reach the active-site serine residue 630 and is involved in the DPPIV activity of CD26 (Rasmussen, et al., 2003). In this regard, this horizontal cavity has an essential role in caveolin-1 binding as well as DPPIV enzyme activity. In particular, CD26 mutants del 201-211 and S630A, in which this cavity was destroyed, had lost the ability to associate with caveolin-1 (Figures 1G, 1H, 3A, and 3B), and did not exert an effect on CD86 upregulation on monocytes (Ohnuma, et al., 2001). In addition, binding of CD26 to caveolin-1 was inhibited by the competitive inhibitor of DPPIV, valine-pyrrolidide (Figures 1H-m, n, o). The valine-pyrrolidide (Val-Pyr) is bound in a smaller pocket within the DPPIV enzymatic active site (Rasmussen, et al., 2003), and two glutamic acids in the horizontal helix of CD26, Glu205 and Glu206, form salt bridges to the free amino group of Val-Pyr. Thus Val-Pyr blocks the accessibility of amino acids to the enzymatic cavity. These findings explain our previous work showing that CD26 lacking DPPIV enzymatic activity could not induce the enhancement of TT-mediated T cell proliferation as well as upregulation of CD86.

One striking feature presented in this study is that caveolin-1 was associated with Tollip in monocytes (Figures 3B-G). It was reported previously that Tollip was involved in

Copy provided by USPTO from the IFW Image Database on 01/11/2005

IL-1R / Toll-like receptor mediated signaling, and that it linked IRAK to NF-κB, JNK and p38 MAP kinase (Cao, et al., 1996; Burns, et al., 2000). Other investigators described that Tollip was associated with Toll-like IL-1R / Toll-like receptor and IRAK complexes, and that removal of Tollip from the complexes would allow signaling to continue by freeing activated IRAK to bind to downstream TRAF6 (Zhang, et al., 2002). Although IRAK was not detected in the complex of caveolin-1 and Tollip (data not shown), CD26 and caveolin-1 were associated, and caveolin-1 was aggregated in the contact area, followed by caveolin-1 phosphorylation. Phosphorylated caveolin-1 subsequently released Tollip presumably due to conformational changes, and Tollip found in the cytoplasm then associated with IRAK for phosphorylation. It remains to be elucidated as to how caveolin-1 and Tollip are linked to IRAK and NF-κB in monocytes.

We next explored the role of the 5'-flanking region of the human CD86 gene in regulating expression of this gene following the interaction of CD26-caveolin-1. The cloning and functional analysis of a 1.3 kilo-base pairs fragment upstream of the transcriptional site of the CD86 gene indicated that two NF-κB binding sites were required for the upregulation of CD86 after CD26-caveolin-1 interaction (Figure 4C). Moreover, in transcription factor assay of TT-loaded monocytes stimulated with CD26, levels of NF-κB (p50 and p65) were detected to be significantly higher than those of STAT-1, or AP-1 (c-Fos, c-Jun) (Figure 4A). In this regard, several other factors, such as IFNγ, TNFα, or CD40-CD154 ligation, were also reported to be involved in the upregulation of CD86 (Berberish, et al., 1994; Li, et al., 1999; Gordon, 2002).

Since loss of caveolae in monocytes was not reported in a caveolin-1 knock-out mouse model (Drab, et al., 2001), and the role and distribution of CD26 in human may be different from that of mouse (Morimoto, et al., 1998), we utilized the RNAi method to analyze directly the function of native caveolin-1 in purified human monocytes. During the past several years, it is shown that RNAi is very effectively utilized in mammalian cells with sequence-specific, small (19- to 22- nucleotides) double strand RNAs (Elbashir, et al., 2001). Although this approach helps to identify the mammalian gene function, one important limitation is that siRNA-based technology only provides a "knock-down" of the targeted protein but not a "knockout". Caveolin-1 is expressed constitutively in monocytes as well as other human tissues including endothelia, fibroblasts, and adipocytes, and treatment of purified human monocytes with siRNA resulted in knockout of caveolin-1 and inhibition of CD86 upregulation following stimulation with CD26-coated beads (Figures 5A-D). Therefore, our findings strongly suggest that caveolin-1 is directly involved in CD86 upregulation in monocytes.

On the basis of our results and previously reported findings, we propose a model to

Copy provided by USPTO from the IFW Image Database on 01/11/2005

describe the signaling events in monocytes triggered by CD26-caveolin-1 interaction (Figure 6A). In this model, caveolin-1 is exposed to cell surface after tetanus toxoid is trafficked in monocytes, and CD26 induces aggregation and phosphorylation of caveolin-1 expressed in T cell-APC contact area, removal of Tollip and subsequent phosphorylation of IRAK. This sequence of events allows for activation of NF-κB and transcription of the CD86 gene. Finally, the induction of CD86 expression and the interaction of CD86 on monocytes and CD28 on T cells resulted in the antigen-specific T cell activation and proliferation. With regards to T cell –APC local interaction and immune response (Figure 6B), entry of recall antigens via caveolae into APC leads to presentation of antigen peptides on MHC class II molecules and exposure of caveolin-1. Then, APC induces the activation of memory T cells through TCR and costimulatory molecules such as CD86/CD80-CD28, leading to formation of mature immunological synapse. Following the association between caveolin-1 on APC and CD26 on memory T cells, CD86 is upregulated on APC surface, and memory T cells are subsequently activated via the costimulatory effect of CD26 on enhancement of TCR activation (Hegen, et al., 1997). By enhancing TCR activation by CD26-caveolin-1 interaction, prolongation of immunological synapse may be maintained (Huppa, et al., 2003). Finally, CD86 upregulation resulted in potent T cell –APC interaction, leading to the development of activated memory T cells locally and activation of the immune response, and the consequence of various inflammatory diseases. Patients with autoimmune diseases such as rheumatoid arthritis, multiple sclerosis and Graves' disease have been found to have increased numbers of $CD26^{high}$ T cells in inflamed tissues as well as in their peripheral blood (Hafler, et al., 1985; Eguchi, et al., 1989; Mizokami, et al., 1996). In addition, enhancement of CD26 expression in these autoimmune diseases may correlate with disease severity. These findings imply that $CD26^{high}$ T cells play a role in the inflammation process and subsequent tissue damage in such diseases. In endothelial cells, inhibition of the scaffolding domain of caveolin-1 reduced inflammation by inhibition of eNOS (endothelial nitric oxide synthase), which was bound to caveolin-1 (Bucci, et al., 2000). Our results may provide a new approach to the treatment of autoimmune diseases or other immune-mediated disorders by directly interfering with activated memory T cell and APC interaction. Moreover, targeting the interaction of the pocket structure of CD26 and the scaffolding domain of caveolin-1 may lead to novel therapeutic approaches utilizing agonists or antagonists regulating antigen-specific immune response in not only immune-mediated disorders, but also cancer immunotherapy and viral vaccination as strategies to enhance immune response.

Copy provided by USPTO from the IFW Image Database on 01/11/2005

Experimental Procedures

Cell lines and Isolation of human monocytes

HEK293 human embryonal kidney, and COS-7 monkey fibroblast cell lines were grown in Dulbecco's Modified Eagle Medium (DMEM) (Sigma-Aldrich, St. Louis, MO) containing 10% fetal calf serum (FCS), 100U/ml penicillin (Life Technologies Inc., Grand Island, NY) and 100 μg/ml streptomycin (Life Technologies Inc.) at 37°C, 5% CO_2. THP-1 human monocyte cell lines were grown in RPMI-1640 medium (Sigma-Aldrich) containing 10% FCS and penicillin-streptomycin at 37°C, 5% CO_2. Jurkat T cell lines with stable expression of CD26 (J.CD26) were cultured in RPMI-1640 medium containing 10% FCS and penicillin-streptomycin, containing 500 μg/ml G418 (Invitrogen, Carlsband, CA) at 37°C, 5% CO_2, as described previously (Tanaka, et al., 1992).

Human peripheral monocytes were purified from peripheral blood mononuclear cells (PBMC), collected from healthy adult volunteers who were immunized with TT within one year before donation according to the methods described previously (Ohnuma, et al., 2001). Monocytes were cultured in Macrophage-SFM medium (Life Technologies Inc.) at 37°C, 5% CO_2, supplemented with penicillin-streptomycin. To avoid interference by non-specific activation of monocytes due to contamination, polymyxin B sulfate (20 IU/ml, Sigma-Aldrich) was added to all media and reagents used for APC/monocytes experiments. Purified monocytes were preincubated in the standard medium for 24 h to minimize the risk of potential interference from sCD26 present in human serum (Tanaka, et al., 1993).

Antibodies and reagents

Anti-human CD26 mouse monoclonal antibody (mAb) (1F7) was developed in our laboratory (Morimoto, et al., 1989). Anti-caveolin-1 rabbit polyclonal antibody (pAb), anti-IRAK rabbit pAb, anti-GST mAb, and Texas red-conjugated anti-immunoglobulin G (Ig) (anti-rabbit-Ig and anti-rat-Ig)) were purchased from Santa Cruz Biotechnology Inc. (Santa Cruz, CA). Anti-phospho-caveolin-1 mAb was obtained from BD Transduction (La Jolla, CA), anti-Tollip rat pAb from ALEXIS Biochemicals (San Diego, CA), and FITC-conjugated anti-CD86, PE-conjugated anti-CD14, Cy Chrome-conjugated anti-CD45 and isotype control mAbs were from BD PharMingen (San Diego, CA). Tetanus toxoid was purchased from Calbiochem (La Jolla, CA), and poly-L-lysin and ADA was from Sigma-Aldrich. Protein labeling with Texas red was made with FluoReporter Texas Red Protein Labeling Kit (Molecular Probes, Eugene, OG) according to the manufacturer's instruction.

Copy provided by USPTO from the IFW Image Database on 01/11/2005

C nstructi ns of plasmids

GST-caveolin-1 and caveolin-1-EGFP were made by inserting caveolin-1 cDNA into pGEX6p1 (Amersham Pharmacia, Piscataway, NJ) and pEB6-CAG-EGFP (kind gift from Dr. Yoshihiro Miwa) (Tanaka, et al., 1999) vectors, respectively. A series of caveolin-1 deletion mutants were made by inserting cDNA fragments of mutated caveolin-1 generated by the polymerase chain reaction (PCR) into pGEX6p1 and pEB6-CAG-EGFP.

CD26-EGFP was made by inserting CD26 cDNA into pEB6-CAG-EGFP. Mutated CD26-EGFP constructions (del201-211) were generated by site-directed mutagenesis method, using the Gene-tailor mutagenesis kit (Invitrogen). GST-CD26 and its deletion mutants were made by inserting CD26 and its mutation cDNA into a mammalian GST expressing vector, pEBG vectors (Sanchez, et al., 1994). The inserted fragments of the deletion mutants (GST-CD26 D1, D 2, D 3) were generated by PCR, and the others (GST-CD26-del 201-211) were constructed by site-directed mutagenesis method using the Gene-tailor mutagenesis kit.

GST-Tollip was made by inserting Tollip cDNA into pGEX6p1. The deletion mutants were constructed by inserting cDNA fragments generated by PCR.

Luciferase chimera of 5'-flanking region of human CD86 gene was generated by inserting PCR fragments of the promoter regions into *Mlu* I-*Xho* I sites of pGL3-basic vector (Promega, Madison, WI). PCR fragments of 5'-flanking region of human CD86 gene was made from ResGen's BAC RPC11 289N10 clone (Invitrogen) as a template with the sense oligos 5'-GGACGCGTTTTAGCATTTTGGTCTAAACTAATTTATAATTATTTAGCCTTA TTTCTCCA-3' (for pGL3-Luc/1181), 5'-GGACGCGTTTGGAATTTAAAATGTTCAAAAT GATTTGT CTGGATG-3' (for pGL3-Luc/783), 5'-GGACGCGTTTGGTTGTGGAAATTGG CAGGGTT AGGTGG-3' (for pGL3-Luc/409), 5'-GGACGCGTATTCAGGCTCATCTTAAC GTCATGTC TGG-3' (for pGL3-Luc/213) and the antisense oligo 5'-CGCTCGAGTGTGCTA GTCCCTGT TACAGCAGC-3'.

All constructs or cDNA fragments were confirmed by DNA sequencing.

Production of GST fusion protein

To produce GST-Caveolin-1, GST-Tollip and their deletion mutants, the plasmid constructs were transformed into BL21 (DE3); pT-Trx *E. coli* (kind gift from Dr. Shun-suke Ishii) (Yasukawa, et al., 1995). GST fusion proteins were induced with 0.1 mM isopropyl-ß-D-thiogalactopyranoside (Amersham Pharmacia) for 10 hrs at 25°C, and purified using Glutathione Sepharose 4B FF (GSH) beads (Amersham Pharmacia).

GST-CD26 and its deletion mutants were produced by the mammalian cell line COS-7. To produce the fusion proteins, 20 μg of pEBG-CD26 or mutants vectors were transfected into $1.0 \cdot 10^7$ COS-7 using Lipofectamine 2000 reagent (Invitrogen), which were

Copy provided by USPTO from the IFW Image Database on 01/11/2005

then grown for 24 hours and lysed on ice with lysis buffer (LB; 1% Nonidet P-40, 130mM NaCl, 20mM Tris-HCl [pH 8.0], 10mM NaF, 2mM sodium orthovanadate [Na_3VO_4], 1% aprotinin, 10μg/ml leupeptin, 1mM phenylmethylsulfonyl fluoride [PMSF], 1 mM EDTA), followed by clarification and incubation of the lysate with GSH beads at 4°C for overnight. The beads were washed three times with LB, twice with 0.5 M LiCl, 20mM Tris-HCl, pH 8.0, and twice with 0.5 M NaCl, 20 mM Tris-HCl, pH 8.0.

The recombinant proteins were obtained by elution from the beads with 10 mM reduced glutathione followed by dialysis in phosphate-buffered saline (PBS). Purification of full-length caveolin-1, mammalian expressed CD26 and its mutant proteins without GST were generated from GST fusion proteins using PreScission protease, followed by dialysis against PBS at 4°C. The predicted sizes of all the expressed proteins were verified by SDS-PAGE.

Purification and separation of CD26 interacting proteins

CD26-bound adenosine deaminase-Sepharose beads (ADA beads) were generated by the methods described previously (Tanaka, et al., 1993; Tanaka, et al., 1994). Total cell lysate of THP-1 monocytes cell lines was applied to the CD26-ADA beads columns. After extensive washes with wash buffer (50 mM Tris-HCl [pH=8.0], 1 mM EDTA, 0.1% NP-40, 50 mM NaCl, 1 mM DTT, 1mM PMSF, 10μg/ml aprotinin), bound proteins were eluted with high-salt buffer (10 mM Tris-HCl [pH 8.0], 1 mM EDTA, 0.1% NP-40, 1000 mM NaCl, 1 mM DTT, 0.5 mM PMSF, 10μg/ml aprotinin).

CD26-ADA beads affinity-purified proteins were separated by SDS-PAGE and stained by silver. Peptide mass mapping was performed by recording peptide mass fingerprints of typic in-gel digests of the corresponding gel bands using MALDI-TOF MS (AXIMA-CFR plus; SHIMADZU BIOTECH, Kyoto, Japan) and subsequently searching the MASCOT database (Matrix Sciences, London, U.K.).

GST pull-down assay

After preclearing by GST on GSH beads, cell lysates were incubated with GST-fused proteins on GSH beads at 4°C for 8 h. Protein-beads complexes were washed extensively with beads with buffer (50 mM Tris-HCl [pH 8.0], 1 mM EDTA, 0.1% NP-40, 50 mM NaCl, 1 mM DTT, 1mM PMSF), and submitted to SDS-PAGE analysis on an appropriate concentration gel under reducing condition using a mini-Protean II system (Bio-Rad Laboratories, Hercules, CA). Proteins were then transferred to a polyvinylidene difluoride membrane (Immobilon-P; Millipore, Bedford, MA). Specific antigens were probed by the corresponding mAbs, followed by HRP-conjugated anti-mouse Ig (Amersham Pharmacia). Western blots were visualized by the enhanced chemiluminescence technique (PerkinElmer Life Science, Boston, MA).

Copy provided by USPTO from the IFW Image Database on 01/11/2005

Cell stimulation

Freshly purified monocytes were cultured in Macrophage-SFM media for 24 h to diminish the effect of serum, and were preincubated with TT at a concentration of 0.5 μg/ml for an additional 24 h. After being washed with PBS, $1.0 \cdot 10^6$ of TT-loaded monocytes were stimulated for indicated periods with $0.5 \cdot 10^6$ particles of polystyrene latex beads (Molecular Probes) coated with rsCD26 wt or rsCD26 del 201-211 (1.0 μg/ml). Stimulated monocytes were subjected to confocal laser microscopy, immunoprecipitation assay, Western blotting analysis, or flow cytometry (FCM).

Freshly isolated T cells, using MACS Pan T cell isolation kit (Mitenyi Biotech, Auburn, CA), were cultured in 10% FCS-RPMI1640 media with PHA (10 ng/ml, Sigma-Aldrich) for 24 h. Thus, activated T cells expressing high levels of CD26 (Morimoto, et al., 1989) were subjected to cell-conjugation assay.

Immunoprecipitation and Western blot analysis

Lyastes were generated with RIPA lysis buffer (1% NP-40, 0.5% sodium deoxycholate, 0.1% SDS, 5mM EDTA, 10mM Tris-HCl (pH 7.4), 0.15 M NaCl, 1mM PMSF, 0.5mM NaF, 10μg/ml aprotinin and 0.02mM Na_3VO_4) from $1.0 \cdot 10^7$ of THP-1 cells incubated with recombinant solubleCD26 (rsCD26) or $1.0 \cdot 10^7$ of TT-loaded monocytes stimulated with rsCD26-coated beads. Then, lysates were clarified by 15,000$\cdot g$ for 30 min. Immunoprecipitates (IPs) were performed by incubating lysates with 2μg of control immunoglobulins (Ig) and protein G-sepharose beads (Amersham Pharmacia) at 4°C for 1 h. After centrifugation, supernatants were incubated with 2μg of specific Ig at 4°C for 2 h, followed by addition of protein G-sepharose beads for an overnight incubation. After washing four times with RIPA lysis buffer, beads were submitted to SDS-PAGE and Western blot analysis.

Confocal laser microscopy

For fluorescent microscopy experiments using HEK293 cells, cells were preincubated in LAB-TEK 4-well chamber slide glass (Nalgen Nunc International, Naperville, IL) for 8 h prior to transfection. GFP fused constructs (GFP-CD26 wt, GFP-CD26 del 201-211, GFP-caveolin-1, or GFP-caveolin-1 del 82-101) were transfected with Lipofectamen 2000 reagent (Invitrogen), and 12 h later, incubated with Texas red conjugated recombinant proteins (caveolin-1 wt, caveloin-1 del 82-101, rsCD26 wt, or rsCD26 del 201-211) for 1 hr. After being washed with ice-cold PBS 3 times, cells were fixed in 4% paraformaldehyde in PBS, followed by mounting with Antifade Prolong kit (Molecular Probes). For blocking experiments using

the competitive DPPIV inhibitor (valine-pyrrolidide (K_i=2.9nM, IC_{50}=13nM), kindly provided by Japan Tobacco Inc., Tokyo, Japan), 1μM of the valine-pyrrolidide was cultured for 15 min with HEK293 cells transfected with GFP fused constructs (GFP-CD26 wt, GFP-CD26 del 201-211, and GFP vector). After repalced fresh 10%-FCS RPMI1640 media, cells were subjected to incuabtion with Texas red conjugated recombinant proteins (caveolin-1 wt or ADA) for 1 h.

For T cell-APC conjugation assay as described elsewhere (Lee, et al., 2002), $1.0 \cdot 10^5$ of activated T cells were mixed with $1.0 \cdot 10^5$ of purified monocytes that had been pulsed with or without TT (0.5 μg/ml for indicated time periods), with further centrifugation. 30 min later, cell mixtures were attached to microslide glass (Matsunami Glass Inc., Tokyo, Japan) coated with poly-L-lysin, and fixed with 4% paraformaldehyde in PBS for 15 min at room temperature. Cells were blocked with mouse and rabbit Ig isotypes (1 μg/ml) for 30 min at 4· , followed by incubation with anti-CD26 mAb and anti-caveolin-1 rabbit pAb (each of 10 μg/ml) for 60 min at 4· , then washed with ice-cold PBS twice and incubated with FITC conjugated anti-mouse Ig and Texas red conjugated anti-rabbit Ig antibodies (1:200) for 60 min at 4· . Cells were mounted in coverslips with Antifade Prolong kit. Conjugates were first identified by direct observation under differential interference contrast and then confirmed by detecting the green fluorescence of anti-CD26 mAb in T cells and the red fluorescence of anti-caveolin-1 pAb in monocytes. The proportion of T cell-APC conjugation was calculated by random choice of 500 different cells in a coverslips from five independent experiments.

For detection of colocalization between caveolin-1 and Tollip, THP-1 cells, which were stably transfected with GFP-caveolin-1, were washed in ice-cold PBS twice, and attached to microslide glass, followed by fixation with acetone-methanol (1:1) for 2 min at room temperature. Then, cells were stained with anti-Tollip rat pAb (10 μg/ml) for 60 min at 4°C, followed by staining with Texas red conjugate anti-rat Ig antibody (1:200) for 60 min at 4· .

Confocal microscopy was performed with an Olympus IX70 confocal microscope with 60 objective lenses (Olympus, Tokyo, Japan), using laser excitation at 496 and 568 nm. The widths of Oregon green and Texas red emission channels were set to maximize specificity.

Flow cytometric analysis

For assessment of cell surface caveolin-1 exposure, after purified monocytes were treated with TT (0.5 μg/ml) for 0, 6, 12, 24, and 48 h, cells were washed with ice-cold PBS three times, and stained with anti-caveolin-1antibody (5 μg/ml) for 60 min at 4°C, followed by staining with FITC conjugated anti-rabbit Ig antibody (1:200) for 60 min at 4°C. To disturb caveolae, purified monocytes were treated with Filipin (1.0 μg/ml, Sigama-Aldrich) for 30 min at 37°C. Cells were then subjected to TT loading and to staining caveolin-1 as described above.

Copy provided by USPTO from the IFW Image Database on 01/11/2005

In experiments assessing the expression of CD86 on purified monocytes after preincubation with or without TT (0.5 μg/ml) for 24 hours, following incubation with rsCD26 –coated beads for 24 h, FITC-conjugated CD86 mAb (10 μg/ml) were used with PE-conjugated anti-CD14 (10 μg/ml) and Cy Chrome-conjugated CD45 (10 μg/ml) to gate exclusively on the monocyte population. In experiments assessing the effect of siRNA against caveolin-1 in monocytes, purified monocytes were transfected with siRNA as described below, following incubation with rsCD26 –coated beads for 24 h, and stained as described above.

Flow-cytometric analysis of 10,000 viable cells was conducted on Becton-Dickinson FACScalibur. Each experiment was repeated at least three times, and the results were provided in the form of a histogram of a representative experiment, or increased mean percent ± standard error (SE) of mean-fluorescent intensity (MFI), compared to control or untreated cells.

Small interfering RNA (siRNA) against caveolin-1

To design target-specific siRNA duplexes, we selected sequences of the type AA(N19) (N, any nucleotide) from the open reading frame of human caveolin-1 (accession number = NM 001753) (Elbashir, et al., 2001). Moreover, we added the sequences to the 2-nucleotide 3' overhangs of 2'-deoxythymidine (dTdT), in order to generate a symmetric duplex with respect to the sequence composition of the sense and antisense 3' overhangs. These symmetric 3' overhangs were reported to help to ensure that the siRNP were formed with approximately equal ratios of sense and antisense target RNA-cleaving siRNP (Elbashir, et al., 2001). Therefore, we selected two target sequences from 81 to 101 (ss1) and 138 to 153 (ss2) downstream of the start codon of caveolin-1 mRNA (sense1 siRNA (ss1-siRNA): 5' AACAACAAGGCCAUGG CAGACdTdT, and sense2 siRNA (ss2-siRNA): 5' AAGGAGA UCGACCUGGUCAAC dTdT). Moreover, mis-siRNA at 4 nucleotides was prepared to examine non-specific effects of siRNA duplexes (mis-siRNA: 5' UACAAGAAGGGCATG GCAGACdTdT). To visualize the efficiency of transfection, we also prepared Texas red-conjugated missense siRNA (mis-siRNA-TR). These selected sequences also were submitted to a BLAST search against the human genome sequence to ensure that only one gene of the human genome was targeted. siRNAs were purchased from QIAGEN (Valencia, CA). Sixty pmole of siRNA duplexes were transfected into $0.5 \cdot 10^6$ cells, using HVJ-E vector (GenomeOne™; kindly provided by IHSIHARA SANGYO KAISHA LTD., Osaka, Japan.). After 24 or 48 h of transfection, cells were prepared for examination.

Luciferase assay

HEK 293cells were plated on 6-cm diameter culture dishes (BD Bioscience, La Jolla, CA) to 30-50% confluence, and cell culture medium was replaced with Opti-MEM medium

(Invitrogen) before transfection. Plasmid mixture was mixed with Lipofectamine 2000 transfection reagent and added to the culture. Total amount of the plasmids was kept constant by adding an irrelevant plasmid. After 6 h of incubation, the medium was replaced with fresh DMEM supplemented with 10% FCS, and the cells were further cultured in the presence or absence of various reagents for 24 h at 37°C. Luciferase enzyme activity was determined using a luminometer (Promega), and relative light units were normalized to the protein amount determined with protein assay reagent according to the manufacturer's instructions (Pierce Biotechnology, Rockford, IL) (Makino, et al., 1996).

Nuclear protein extraction and DNA-binding protein assay

Nuclear protein extraction (NE) was obtained with TransFactor Extraction Kit (Clontech, Palo Alto, CA) from purified monocytes which were treated with TT, followed by rsCD26 stimulation. Each 6 μg NE (with or without the specific competitor oligos (500 ng)) was subjected to ELIZA-based DNA-binding protein assay, using Mercury TransFactor Kit (Clontech). DNA-binding protein activity was measured by the absorbance value at 655nm with microtiter plate reader (Bio-Rad) with reference at 405 nm.

Statistics

Student's *t* test was used to determine whether the difference between control and sample was significant ($p < 0.05$ being significant).

Any publications cited herein are incorporated by reference.

Copy provided by USPTO from the IFW Image Database on 01/11/2005

References

- Azuma, M., Ito, D., Yagita, H., Okumura, K., Phillips, J.H., Lanier, L.L., and Somoza, C. (1993). B70 antigen is a second ligand for CTLA-4 and CD28. Nature *366*, 76-79.

- Berberish, I., Shu, G.L., and Clark, E.A. 1994. Cross-linking CD40 on B cells rapidly activates nuclear factor-• B. J Immunol. *153*, 4357-4366.

- Bucci, M., Gratton, J.P., Rudic, R.D., Acevedo, L., Roviezzo, F., Cirino, G., and Sessa, W.C. (2000). In vivo delivery of the caveolin-1 scaffolding domain inhibits nitric oxide synthesis and reduces inflammation. Nature Med. *6*, 1362-1367.

- Burns, K., Clatworthy, J., Martin, L., Martinon, F., Plumpton, C., Maschera, B., Lewis, A., Ray, K., Tschopp, J., and Volpe, F. (2000). Tollip, a new component of the IL-1RI pathway, links IRAK to the IL-1 receptor. Nature Cell Biol. *2*, 346-351.

- Cao, Z., Henzel, W.J., and Gao, X. (1996). IRAK: a kinase associated with interleukin-1 receptor. Science *271*, 1128-1131.

- Carver, L.A., and Schnitzer, J.E. (2003). Caveolae. Mining little caves for new cancer target. Nature Rev. Cancer. *3*, 571-581.

- Caux, C., Vanbervliet, B., Massacrier, C., Azuma, M., Okumura, K., Lanier, L.L., and Banchereau, J. (1994). B70/B7-2 is identical to CD86 and is the major functional ligand for CD28 expressed on human dendritic cells. J. Exp. Med. *180*, 1841-1847.

- Chambers, C.A. (2001). The expanding world of co-stimulation: the two-signal model revisited. Trends Immunol. *22*, 217-223.

- Croft, M., Duncan, D.D., and Swain, L.S. (1992). Response of naive antigen-specific CD4+ T cells in vitro: characteristics and antigen-presenting cell requirements. J. Exp. Med. *176*, 1431-1437.

- Drab, M., Verkade, P., Elger, M., Kasper, M., Lohn, M., Lauterbach, B., Menne, J., Lindschau, C., Mende, F., Luft, F.C., Schedl, A., Haller, H., and Kurzchalia, T.V. (2001). Loss of caveolae, vascular dysfunction, and pulmonary defects in caveolin-1 gene-disrupted mice. Science *293*, 2449-5242.

- Eguchi, K., Ueki, Y., Shimomura, C., Otsubo, T., Nakao, H., Migita, K., Kawakami, A., Matsunaga, M., Tezuka, H., Ishikawa, N., and Nagatuki, S. (1989). Increment in the Ta1+ cells in the peripheral blood and thyroid tissue of patients with Graves' disease. J. Immunol. *142*, 4233-4240.

- Elbashir, S.M., Harborth, J., Lendeckel, W., Yalcin, A., Weber, C., and Tuschl, T. (2001). Duplexes of 21-nucleotide RNAs mediate RNA interference in cultured mammalian cells. Nature *411*, 494-498.

- Fleischer, B. (1994). CD26: surface protease involved in T-cell activation. Immunol. Today *15*, 180-184.

- Fraser, J.D., and Weiss, A. (1992). Regulation of T-cell lymphokine gene transcription by the accessory molecule CD28. Mol Cell Biol. *12*, 4357-4363.

- Freeman, G.J., Gribben, J.G., Bousiotis, V.A., Ng, J.W., Restivo, V.A., Lombard, L.A., Gray, G.S., and Nadler, L.M. (1993). Cloning of B7-2: a CTLA-4 counter-receptor that costimulates human T cell proliferation. Science *262*, 909-911.

- Galbiati, F., Razani, B., and Lisanti, M.P. (2001). Emerging themes in lipid rafts and caveolae. Cell *106*, 403-411.

- Gordon, S. (2002). Alternative activation of macrophages. Nature Rev. Immunol. *3*, 23-35.

- Grakoui, A., Bromley, S.K., Sumen, C., Davis, M.M., Shaw, A.S., Allen, P.M., Dustin, M.L. (1999). The immunological synapse: a molecular machine controlling T cell activation. Science *285*, 221-227.

- Hafler, D.A., Fox, D.A., Manning, M.E., Schlossman, S.F., Reinherz, E.L., and Weiner, H.L. (1985). In vivo activated T lymphocytes in the peripheral blood and cerebrospinal fluid of patients with multiple sclerosis. N. Engl. J. Med. *312*, 1405-1411.

- Hakamada-Taguchi, R., Kato, T., Ushijima, H., Murakami, M., Uede, T., and Nariuchi, H. (1998). Expression and co-stimulatory function of B7-2 on murine CD4+ T cells. Eur. J. Immunol. *28*, 865 873.

- Hathcock, K.S., Laszlo, G., Pucillo, C., Linsley, P., and Hodes, R.J. (1994). Comparative analysis of B7-1 and B7-2 costimulatory ligands: expression and function. J. Exp. Med. *180*, 631-640.

- Hegen, M., Kameoka, J., Dong, R-P., Schlossman, S.F., and Morimoto, C. (1997). Cross-linking of CD26 by antibody induces tyrosine phosphorylation and activation of mitogen-activated protein kinase. Immunology *90*, 257-264.

- Huppa, J.B., Gleimer, M., Sumen, C., and Davis, M.M. (2003). Continuous T cell receptor signaling required for synapse maintenance and full effector potential. Nature Immunol. *4*, 749-755.

- Ikushima, H., Munakata, Y., Ishii, T., Iwata, S., Terashima, M., Tanaka, H., Schlossman, S.F., and Morimoto, C. (2000). Internalization of CD26 by mannose 6-phosphate/insulin-like growth factor II receptor contributes to T cell activation. Proc. Natl. Acad. Sci. USA. *97*, 8439-8444.

- Iwata, S., Yamaguchi, N., Munakata, Y., Ikushima, H., Lee, J.F., Hosono, O., Schlossman, S.F., and Morimoto, C. (1999). CD26/dipeptidyl peptidase IV differentially regulates the chemotaxis of T cells and monocytes toward RANTES: possible mechanism for the switch from innate to acquired immune response. Int. Immunol. *11*, 417-426.

- Kameoka, J, Tanaka, T., Nojima, Y., Schlossman, S.F., and Morimoto, C. (1993). Direct association of adenosine deaminase with a T cell activation antigen, CD26. Science *261*, 466-469.

Copy provided by USPTO from the IFW Image Database on 01/11/2005

- Krummel, M.F., and Allison, J.P. (1995). CD28 and CTLA-4 have opposing effects on the response of T cells to stimulation. J. Exp. Med. *182*, 459-465, 1995.
- Lee K.H., Holdorf, A.D., Dustin, M.L., Chan, A.C., Allen, P.M., and Shaw, A.S. (2002). T cell receptor signaling precedes immunological synapse formation. Science *295*, 1539-1542.
- Lenschow, D.J., Walunas, T.L., and Bluestone, J.A. (1996). CD28/B7 system of T cell costimulation. Annu. Rev. Immunol. *14*, 233-258.
- Li, J., Liu, Z., Jiangu, S., Cortesini, R., Lederman, S., and Suciu-Foca, N. (1999). T suppressor lymphocytes inhibit NF-κB -mediated transcription of CD86 gene in APC. J. Immunol *163*, 6386-6392.
- Makino, Y., Okamoto, K., Yoshikawa, N., Aoshima, M., Hirota, K., Yodoi, J., Umesono, K., Makino, I., and Tanaka, H. (1996). Thioredoxin: a Redox-regulating Cellular Cofactor for Glucocorticoid Hormone Action Cross Talk between Endocrine Control of Stress Response and Cellular Antioxidant Defense System. J. Clin. Invest. *98*, 2469-2477.
- Manickasingham, S.P., Anderson, S.M., Burkhart, C., and Wraith, D.C. (1998). Qualitative and quantitative effects of CD28/B7-mediated costimulation on naive T cells in vivo. J. Immunol. *161*, 3827-3835.
- McAdam, A.J., Schweitzer, A.N., and Sharpe, A.H. (1998). The role of B7 co-stimulation in activation and differentiation of CD4+ and CD8+ T cells. Immunol. Rev. *165*, 231-247.
- Medzhitov, R. (2001). Toll-like receptors and innate immunity. Nature Rev. Immunol. *1*, 135-145.
- Mizokami, A., Eguchi, K., Kawakami, A., Ida, H., Kawabe, Y., Tsukada, T., Aoyagi, T., Maeda, K., Morimoto, C., and Nagataki, S. (1996). Increased population of high fluorescence 1F7 (CD26) antigen on T cells in synovial fluid of patients with rheumatoid arthritis. J. Rheumatol. *23*, 2022-2026.
- Montesano, R., Roth, J., Robert, A., and Orchi, L. (1982). Non-coated membrane invaginations are involved in binding and internalization of cholera and tetanus toxins. Nature *296*, 651-653.
- Morimoto, C., Torimoto, Y., Levinson, G., Rudd, C.E., Schrieber, M., Dang, N.H., Letvin, N.L., and Schlossman, S.F. (1989). 1F7, a novel cell surface molecule involved in helper function of CD4 cells. J. Immunol. *143*, 3430-3439.
- Morimoto, C., and Schlossman, S.F. (1998). The structure and function of CD26 in the T-cell immune response. Immunol. Rev. *161*, 55-70.
- Ohnuma, K., Munakata, Y., Ishii, T., Iwata, S., Kobayashi, S., Hosono, O., Kawasaki, H., Dang, N.H., and Morimoto, C. (2001). Soluble CD26/dipeptidyl peptidase IV induces T cell proliferation through CD86 up-regulation on APCs. J. Immunol. *167*, 6745-6755.
- Oravecz, T., Pall, M., Roderiquez, G., Gorrell, M.D., Ditto M., Nguyen, N.Y., Boykins, R.,

Copy provided by USPTO from the IFW Image Database on 01/11/2005

Unsworth, E., and Norcross, M.A. (1997). Regulation of the receptor specificity and function of the chemokine RANTES (Regulated on Activation, Normal T cells Expressed and Secreted) by dipeptidyl peptidase IV (CD26)-mediated cleavage. J. Exp. Med. *186*, 1865-1872.

- Peiro, S., Comella, J.X., Enrich, C., Martin-Zanca, D., and Rocamora, N. (2000). PC12 cells have caveolae that contain TrkA, Caveolae-disrupting drugs inhibit nerve growth factor-induced, but not epidermal growth factor-induced, MAPK phosphorylation. J. Biol. Chem. *275*, 37846-37852.

- Pelkmans, L., and Helenius, A. (2002). Endocytosis via caveolae. Traffic *3*, 311-20.

- Rasmussen, H.B., Branner, S., Wiberg, F.C., and Wagtoman, N. (2003). Crystal structure of human dipeptidyl peptidase IV/CD26 in complex with a substrate analog. Nature Struct. Biol. *10*, 19-25.

- Riemann, D., Hansen, G.H., Niels-Christiansen, L.L., Thorsen, E., Immerdal, L., Santos, A.N., Kehlen, A., Langner, J., and Danielsen, E.M. (2001). Caveolae/lipid rafts in fibroblast-like synoviocytes: ectopeptidase-rich membrane microdomains. Biochem. J. *354*, 47-55.

- Sanchez, I., Hughes, R.T., Mayer, B.J., Yee, K., Woodgett, J.R., Avruch, J., Kyriakis, J.M., and Zon, L.I. (1994). Role of SAPK/ERK kinase-1 in the stress-activated pathway regulating transcription factor c-Jun. Nature *372*, 794-798.

- Smart, E.J., Graf, G.A., McNiven, M.A., Sessa, W.C., Engleman, J.A., Sherper, P.E., Okamoto, T., and Lisanti, M.P. (1999). Caveolins, liquid-ordered domains, and signal transduction. Mol. Cell Biol. *19*, 7289-7304.

- Tanaka, T., Camerini, D., Seed, B., Torimoto, Y., Dang, N.H., Kameoka, J., Dahlberg, H.N., Schlossman, S.F., and Morimoto, C. (1992). Cloning and functional expression of the T cell activation antigen CD26. J. Immunol. *149*, 481-486.

- Tanaka, T., Kameoka, J., Yaron, A., Schlossman, S.F., and Morimoto, C. (1993). The costimulatory activity of the CD26 antigen requires dipeptidyl peptidase IV enzymatic activity. Proc. Natl. Acad. Sci. USA. *90*, 4583-4590.

- Tanaka, T., Duke-Cohan, J.S., Kameoka, J., Yaron, A., Lee, I., Schlossman, S.F., and Morimoto, C. (1994). Enhancement of antigen-induced T-cell proliferation by soluble CD26/dipeptidyl peptidase IV. Proc. Natl. Acad. Sci. USA. *91*, 3082-3086.

- Tanaka, J., Miwa, Y., Miyoshi, K., Ueno, A., and Inoue, H. (1999). Construction of Epstein-Barr virus-based expression vector containing MiniOriP. Biochem. Biophy. Res. Com. *264*, 938-943.

- Turley, S.J., Inaba, K., Garrett, W.S., Ebersold, M., Unternaehrer, J., Steinman, R.M., and Mellman, I. (2000). Transport of peptide-MHC class II complexes in developing dendritic cells. Science *288*, 522-527.

- von Bonin, A., Huhn, J., and Fleischer, B. (1998). Dipeptidyl-peptidase IV/CD26 on T cells:

Copy provided by USPTO from the IFW Image Database on 01/11/2005

analysis of an alternative T-cell activation pathway. Immunol. Rev. *161*, 43-53.

- Walunas, T.L., Lenschow, D.J., Bakker, C.Y., Linsley, P.S., Freeman, G.J., Green, J.M., Thompson, C.B., and Bluestone, J.A. (1994). CTLA-4 can function as a negative regulator of T cell activation. Immunity *1*: 4405-413.

- Yasukawa, T., Kanei-Ishii, C., Maekawa, T., Fujimoto, J., Yamamoto, T., and Ishii, S. (1995). Increase of solubility of foreign proteins in *Escherichia Coli* by coproduction of the bacterial thioredoxin. J. Biol. Chem. *270*, 25328-25331.

- Yi-qun, Z., Joost van Neerven, R.J., Kasran, A., de Boer, M., and Ceuppens, J.L. (1996). Differential requirements for co-stimulatory signals from B7 family members by resting versus and recently activated memory T cells towards soluble recall antigens Int. Immunol. *8*, 37-44.

- Yokochi, T., Holly, R.D., and Clark, E.A. (1982). B lymphoblast antigen (BB-1) expressed on Epstein-Barr virus-activated B cell blasts, B lymphoblastoid cell lines, and Burkitt's lymphomas. J. Immunol. *128*, 823-827.

- Zhang, G., and Ghosh, S. (2002). Negative regulation of Toll-like receptor-mediated signaling by Tollip. J. Biol. Chem. *277*, 7059-7065.

Legends to Figures

Figure 1. Purification and identification of CD26-binding proteins. (A) The indicated fractions were subjected to SDS-PAGE followed by silver staining. Total cell lysate (Lysate) of THP-1 cells, an eluted fraction from mock purification (ADA beads), a flow-through fraction (Washout) from an eluted fraction of CD26-ADA sepharose column for THP-1 cells (Elution). Proteins eluted from CD26-ADA sepharose columns were identified by MS analysis, indicated on the right. (B) THP-1 cells cocultured with soluble CD26 (sCD26) were immunoprecipitated (IP) with either anti-caveolin-1 (right panel) or anti-CD26 antibodies (left panel). Immune complexes were resolved by SDS-PAGE and immunoblotted with anti-CD26 or anti-caveolin-1. Membranes were stripped and reprobed with the indicated antibodies. (C) Schematic representation of the bacterially produced GST-fused caveolin-1 and its mutants. Residues 1-81 comprised the N-terminal region (right dotted square), residues 82-101 comprised the scaffolding domain (SCD) (black square), residues 102-134 comprised the transmembrane region (striped square), and residues 135-178 comprised the C-terminal region (left dotted square). (D) GST-fused caveolin-1 and its mutants on gluthatione sepharose (GSH) beads were incubated with J.CD26 cell lysate after preclearing with GST on GSH beads. Bound proteins and 1% amount of input lysate were resolved by SDS-PAGE and immunoblotted with anti-CD26 antibody, followed by stripping and reprobing with anti-GST antibody. (E) Texas red conjugated sCD26 (rsVD26 Texas red) was incubated with HEK293 cells transfected with GFP-fused wild type caveolin-1 (wt) (a-c), deletion mutant lacking the SCD (del 82-101) (d-f), and GFP vector alone (g-i). Cells were visualized with confocal laser microscopy. Bars indicate 10 μm scale. (F) Schematic representation of the GST-fused CD26 and its deletion mutants, produced by COS-7 cells and purified with GSH beads. Transmembrane and cytosolic regions were deleted. Residues 201-211 contain a caveolin-binding domain (CBD). To delete DPPIV enzymatic activity, serine at residue 630 was mutated for alanine residue (S630A). (G) GST-fused CD26 and deletion mutants on GSH beads were incubated with THP-1 cell lysate after preclearing with GST on GSH beads. Bound proteins and 1% amount of input lysate were resolved by SDS-PAGE and immunoblotted with anti-caveolin-1 antibody, followed by stripping and reprobing with anti-GST antibody. (H) Texas red conjugated caveolin-1 was incubated with HEK293 cells transfected with GFP-fused wild type CD26 (wt) (a-c), deletion mutant lacking the CBD (del 201-211) (d-f), DPPIV activity-deleted mutant (S630A) (h-i) and GFP vector alone (j-l). HEK293 cells transfected with GFP-fused wild type CD26 (wt) were incubated with DPPIV inhibitor valine-pyrrolidide (Val-Pyr) prior to adding Texas red conjugated caveolin-1 (m-o). To confirm CD26 binding activity other than DPPIV-related molecules, Texas red conjugated ADA was added to HEK293 cells transfected with GFP-fused wild type CD26 (wt) which were incubated with Val-Pyr (p-r). Cells were visualized with

Copy provided by USPTO from the IFW Image Database on 01/11/2005

confocal laser microscopy. Bars indicate 10 μm scale.

Figure 2. Caveolin-1 in monocytes was exposed to cell surface after tetanus toxoid (TT) treatment, and interacted with CD26 on activated T cells. **(A)** After purified monocytes were incubated with (solid circle) or without (open circle) TT for the indicated time periods, cell surface caveolin-1 was stained with anti-caveolin-1 antibody detecting the N terminal region, followed by staining with anti-rabbit Ig FITC, and analyzed for %positive cells by flow cytometry. For inhibition study of caveolae formation, purified monocytes were preincubated with Filipin for 30 min, followed by incubation with (solid triangle) or without (open triangle) TT for the indicated time periods, and then cell surface caveolin-1 was detected by the same method as described above. Data of %positive cells represent mean ± standard errors (SE) from five independent experiments. Asterisks indicate points of significant increase. Representative numbers of mean fluorescence intensity (MFI) of caveolin-1 in TT-loaded monocytes were shown. **(B)** Without centrifugation after mixing, activated T cells and TT-loaded monocytes were attached to coverslips, fixed without permeabilization, stained with anti-CD26 (FITC) and anti-caveolin-1 (Texas red) antibodies. In these experiments, CD26 was detected exclusively on activated T cells (a), and cell surface caveolin-1 was detected exclusively on TT-loaded monocytes (b, c). Bars indicate 10 μm scale. **(C)** To form cell-cell conjugation, activated T cells and 24-hour TT-loaded monocytes were mixed, followed by centrifugation. Following incubation for 30 min, conjugates were attached to coverslips, fixed without permeabilization, stained with anti-CD26 (FITC) and anti-caveolin-1 (Texas red) antibodies. Three representative conjugates were shown (conj#1-#3). Bars indicate 10 μm scale. **(D)** Quantification of cell conjugation between T cells and monocytes as shown in Figure 2C. After purified monocytes were incubated with (solid circle) or without (open circle) TT for the indicated time periods, T cell-monocyte conjugation was formed and stained as described in Experimental Procedures. For inhibition study of caveolae formation, purified monocytes were preincubated with Filipin for 30 min, followed by incubation with (solid triangle) or without (open triangle) TT for the indicated time periods, and then subjected to T cell-monocyte conjugation assay by the same method as described above. Data represent mean ± SE of T cell-monocyte conjugation frequency in 500 random cells in a coverslip analyzed in five independent experiments. Asterisks indicate points of significant increase.

Figure 3. CD26 induced phosphorylation of caveolin-1 in TT-loaded monocytes, followed by release of Tollip to phosphorylate IRAK. **(A)** TT-loaded monocytes were incubated with polystyrene latex beads coated with wild type CD26 (wt) (a) or deletion mutant CD26 lacking the CBD (del201-211) (b). After attachments to coverslips, conjugates were fixed without

Copy provided by USPTO from the IFW Image Database on 01/11/2005

permeabilization and stained with anti-caveolin-1 antibody, followed by staining with anti-rabbit Ig FITC antibody. Cells and beads were visualized by confocal laser microscopy. Panels were phase contrast photos merged with FITC views. Bars indicate 10 μm scale. **(B)** TT-loaded monocytes were stimulated with CD26 (wt) coated beads for the indicated time periods. Cell lysates were immunoprecipitated (IP) with anti-caveolin-1 antibody, and immune complexes were resolved by SDS-PAGE, immunoblotted with anti-phospho-caveolin-1 or anti-Tollip antibodies, followed by stripping and reprobing with anti-caveolin-1 antibody. Total cell lysates were also resolved by SDS-PAGE, immunoblotted with anti-IRAK antibody. Position of IRAK bands was indicated by open arrow heads, and supershifted bands of IRAK was indicated by solid arrow head. The reciprocal intensities of phospho-caveolin (open bars) and Tollip (solid bars) immunoprecipitated by anti-caveolin-1 were demonstrated. **(C)** TT-loaded monocytes were stimulated with CD26 (del201-211) coated beads for the indicated time periods. IP and Western blot analyses were performed as described in (B). The reciprocal intensities of phospho-caveolin (open bars) and Tollip (solid bars) immunoprecipitated by anti-caveolin-1 were demonstrated. **(D)** THP-1 cells transfected with GFP-caveolin-1 were stained with anti-Tollip and anti-rat-Ig Texas red antibodies, and visualized by confocal laser microscopy. Bars indicate 10 μm scale. **(E)** GST-fused caveolin-1 and deletion mutants on GSH beads were incubated with THP-1 cell lysate after preclearing with GST on GSH beads. Bound proteins and 1% amount of input lysate were resolved by SDS-PAGE and immunoblotted with anti-Tollip antibody, followed by stripping and reprobing with anti-GST antibody. **(F)** Schematic representation of the bacterially produced GST-fused Tollip and deletion mutants. Residues 47-178 (black square) were the C2 regions (protein kinase C conserved region 2), and residues 178-274 (left gray square) were the CUE domain (ubiquitin-conjugating enzyme binding domain). **(G)** GST-fused Tollip and deletion mutants on GSH beads were incubated with THP-1 cell lysate after preclearing with GST on GSH beads. Bound proteins and 1% amount of input lysate were resolved by SDS-PAGE and immunoblotted with anti-caveolin-1 antibody, followed by stripping and reprobing with anti-GST antibody.

Figure 4. CD26 stimulation on TT-loaded monocytes activated NF-κB to upregulate CD86. **(A)** TT-loaded monocytes were stimulated with CD26-coated beads for 2 hours or PMA, and harvested for extraction of nuclear proteins (NE). Each 6 μg of NE with or without the specific competitor oligos was subjected to ELIZA-based DNA-binding protein assay. Binding activity was revealed by OD value at 655 nm. Data represent mean ± SE from triplicate experiments. Asterisks show points of significant increase. **(B)** Schematic representation of luciferase chimera constructs of the 5'-flanking region of human CD86 gene and deletion mutants. The

Copy provided by USPTO from the IFW Image Database on 01/11/2005

two GAS elements (gamma-interferon activation sites) at –1187 and –1127 are shown by filled circle, and the two NF-κB sites at –612 and –238 are filled triangle. The position of each construct relative to the transcription start site (+1) is indicated. (C) 12 hrs after HEK293 cells were cotransfected with CD86-promoter luciferase constructs and wild type caveolin-1 expressing vectors, wild type soluble CD26 (rsCD26 wt) or mutant rsCD26 del 201-211, lacking 201-211 residues, was added to the culture media, and incubated for an additional 20 hrs. Cells were harvested for measurement of luciferase activity and protein concentration. Luciferase activity is shown as being relative to one μg of applied protein. Data represent mean ± SE from triplicate experiments. Asterisks indicate points of significant increase. (D) 12 hrs after HEK293 cells were cotransfected with pGL3-Luc/1181 or pGL3-Luc/basic, and wild type caveolin-1 expressing vectors, various concentrations of wild type soluble CD26 (rsCD26 wt) or mutant rsCD26 del 201-211, lacking 201-211 residues, were added to the culture media, and incubated for an additional 20 hrs. Cells were harvested for measurement of luciferase activity and protein concentration. Luciferase activity is shown as being relative to one μg of applied protein. Data represent mean ± SE from triplicate experiments.

Figure 5. siRNA against caveolin-1 inhibited effect of CD26 on CD86 upregulation in TT-loaded monocytes. (A) Purified monocytes were transfected with Texas red conjugated mismatched siRNA, using HVJ-E vector. After 24 hrs of transfection, cells were attached to coverslips, fixed, stained with anti-CD14-FITC, and visualized by confocal laser microscopy. (B) Purified monocytes were transfected with or without sense-siRNA (ss1 is targeted for +81 to +101 of caveolin-1 gene and ss2 for +138 to +158) or mismatched siRNA, using HVJ-E vector. 48 hrs later after transfection, cell lysates were prepared, resolved by SDS-PAGE, immunobloted with anti-caveolin-1 antibody, followed by stripping and reprobing with anti-ß-actin antibody. The reciprocal intensities of caveolin-1 to ß-actin were demonstrated by bar graph. (C) Purified monocytes were transfected with or without siRNA using HVJ-E vector, followed by treatment with TT. After stimulation with CD26-coated beads, cells were subjected to analysis of surface CD86 expression by FCM. Monocytes were identified by gating of CD45-Cy Chrome and CD14-PE positive population. The representative histograms are shown from 5 independent experiments. Arrow heads indicate strong positive area. (D) Mean fluorescence intensity (MFI) of cell surface CD86 as studied in (C) are demonstrated. Data represent mean ± SE of five independent experiments. ** indicates points of no significant change by sense siRNA, whereas * shows points of significant increase.

Figure 6. Model for CD26-caveolin-1 interaction leading to immune enhancement. (A) (1) Caveolin-1 in monocytes (APC) resides at the inner membrane with or without Tollip presence.

Copy provided by USPTO from the IFW Image Database on 01/11/2005

(2) After uptake of tetanus toxoid into monocytes via caveolae, some population of caveolin-1 flip-flop to be exposed on the outer cell surface of TT-loaded monocytes. (3) Migration of CD26 positive activated T cells to areas of antigen-loaded APCs results in contact with TT antigen-presenting APC and formation of immunological synapse, leading to association of CD26 and caveolin-1. Caveolin-1 is aggregated in contact area, followed by its phosphorylation. (4) Phosphorylated caveolin-1 (phospho-caveolin-1) releases complexed Tollip, presumably due to conformational changes, and Tollip in the cytosol then interacts with IRAK. (5) After IRAK is phosphorylated, NF-κB is activated to lead to upregulation of CD86. (B) T cell –APC local interaction and immune response. (1) entry of recall antigens via caveolae into APC leads to presentation of antigen peptides on MHC class II molecules and exposure of caveolin-1. (2) Through formation of mature immunological synapse, APC stimulates memory T cell through TCR and costimulatory molecules such as CD86/CD80-CD28. At one time, caveolin-1 on APC is associated with CD26 on memory T cell, and CD86 is upregulated in APC and memory T cell is activated via CD26 costimulatory effect. (3, 4) CD86 upregulation results in greater T cell –APC interaction, which then leads to the development of memory activated T cells locally and activated immune response, resulting in potential autoimmune diseases, etc.

Copy provided by USPTO from the IFW Image Database on 01/11/2005

What is claimed is:

1. A method for treating a disease in need of downregulation of immune response, wherein said method comprises administering a substance that inhibits the binding between CD26/dipeptidyl peptidase IV (DPPIV) and caveolin-1 in a patient in need of the treatment.

2. The method of claim 1, wherein said substance targets a pocket structure of amino acid residues at 201 to 211 of CD26 or the DPPIV enzymatic active site of a serine residue at 630 of CD26.

3. The method of claim 1, wherein said substance is a DPPIV inhibitor.

4. The method of claim 4, wherein said DPPIV inhibitor is valine-pyrrolidide.

5. The method of claim 1, wherein said substance targets a scaffolding domain of amino acid residues at 82 to 101 of caveolin-1.

6. The method of claim 1, wherein said substance is a caveolae trafficking inhibitor.

7. The method of claim 6, wherein said substance is filipin.

8. The method of claim 1, wherein said substance inhibits the expression of caveolin-1.

9. The method of claim 8, wherein said substance is small interfering (siRNA) against caovelin-1.

10. The method of claim 9, wherein said siRNA having a nucleotide sequence of AACAACAAGGCCAUGGCAGACdTdT or AAGGAGAUCGACCUGGUCAACdTdT.

11. The method of claim 1, wherein said disease is an inflammatory disease, an autoimmune disease, other immune-mediated disorder, or organ transplantation.

12. A method for treating a disease in need of upregulation of immune response, wherein said method comprises administering a substance that upregulates CD26 or caveolin-1 to a patient in need of the treatment.

13. The method of claim 12, wherein said treatment is viral vaccination or cancer therapy selected from immunotherapy and suppression of metastasis.

14. A method of screening a substance that downregulates immune response, wherein the method comprises:

trasfecting a cell with CD26 labeled with a detection marker, wherein said

Copy provided by USPTO from the IFW Image Database on 01/11/2005

cell does not express CD26 and caveolin-1;

contacting a test sample with the CD26-transfected cell;

adding caveolin-1 to the cell, wherein said caveolin-1 is labeled with another detection marker;

detecting the labels of CD26 and caveolin-1 in the cell; and

selecting a test sample that has made only the label of caveolin-1 undetectable.

Copy provided by USPTO from the IFW Image Database on 01/11/2005

This Page Is Inserted by IFW Operations
and is not a part of the Official Record

BEST AVAILABLE IMAGES

Defective images within this document are accurate representations of the original documents submitted by the applicant.

Defects in the images may include (but are not limited to):

- BLACK BORDERS
- TEXT CUT OFF AT TOP, BOTTOM OR SIDES
- FADED TEXT
- ILLEGIBLE TEXT
- SKEWED/SLANTED IMAGES
- COLORED PHOTOS
- BLACK OR VERY BLACK AND WHITE DARK PHOTOS
- GRAY SCALE DOCUMENTS

IMAGES ARE BEST AVAILABLE COPY.

As rescanning documents *will not* correct images, please do not report the images to the Image Problem Mailbox.

Scanned with USPTO from the IFW Image Database on 01/11/2006

Figure 1

A

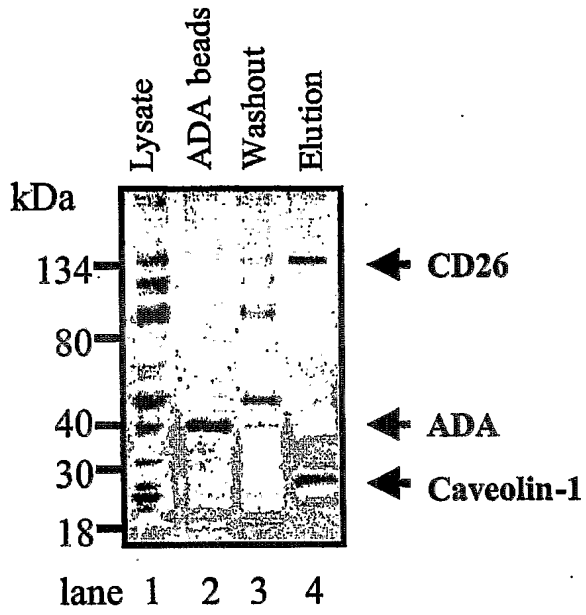

B

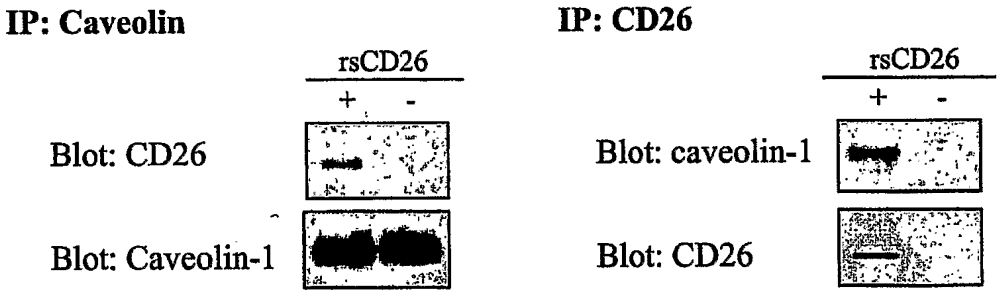

C

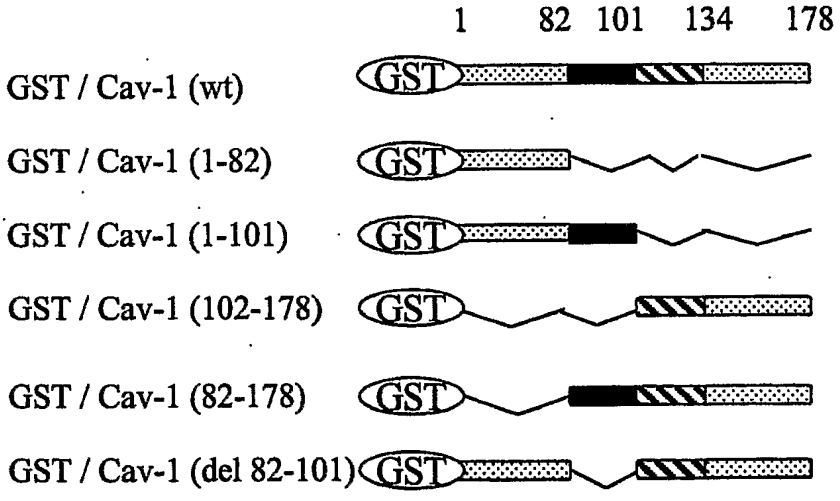

Provided by USPTO from the IFW Image Database on 01/11/2005

Figure 1

D

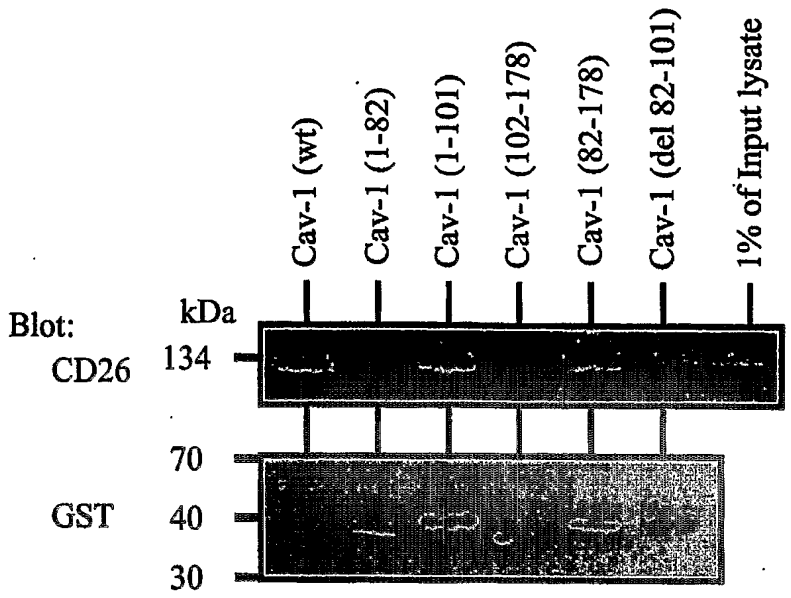

E

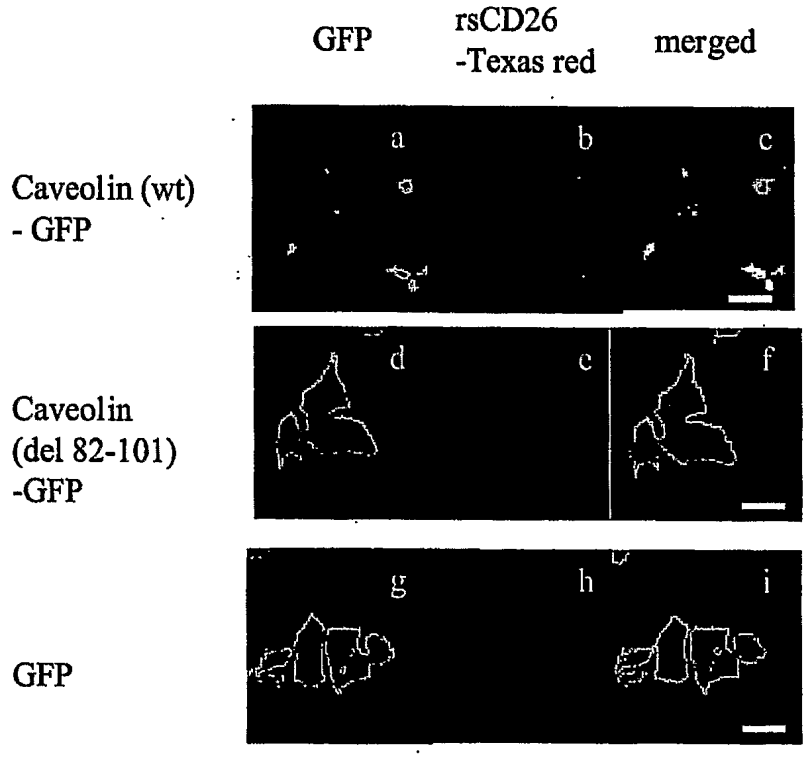

Copy provided by USPTO from the IFW Image Database on 01/11/2005

Figure 1

F

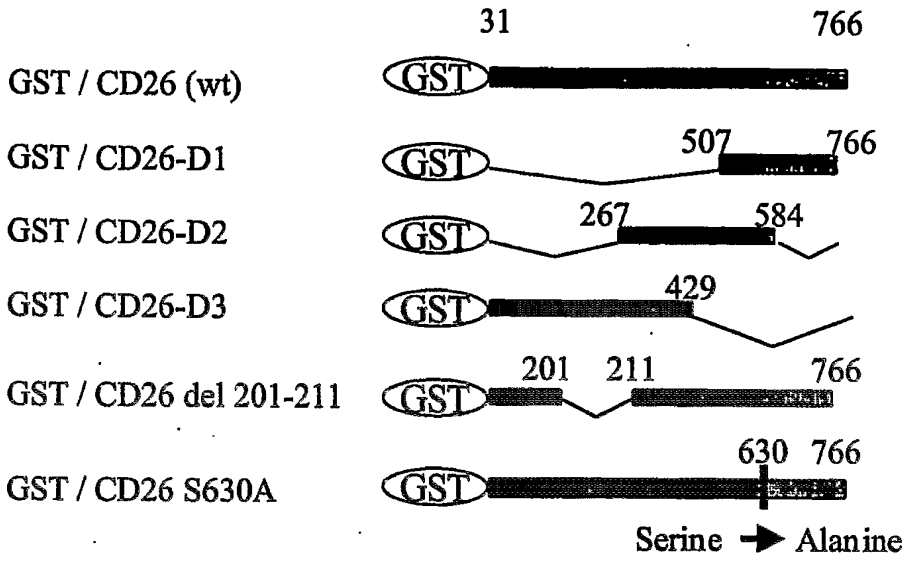

G

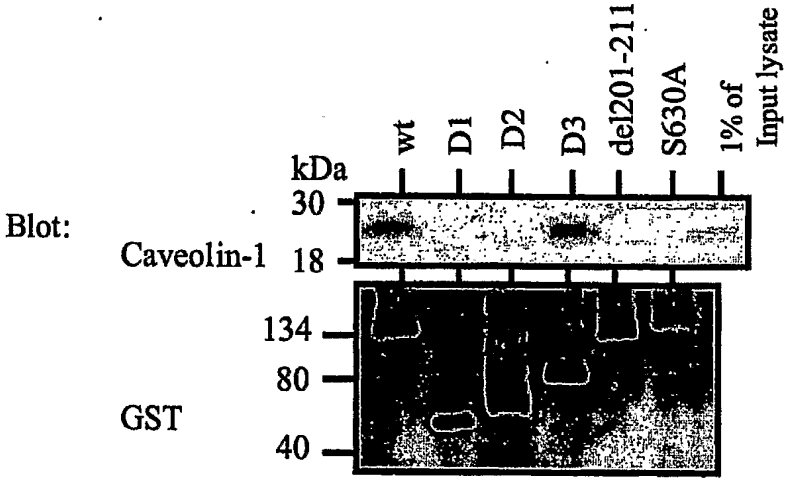

Copy provided by USPTO from the IFW Image Database on 01/11/2005

Figure 1

H

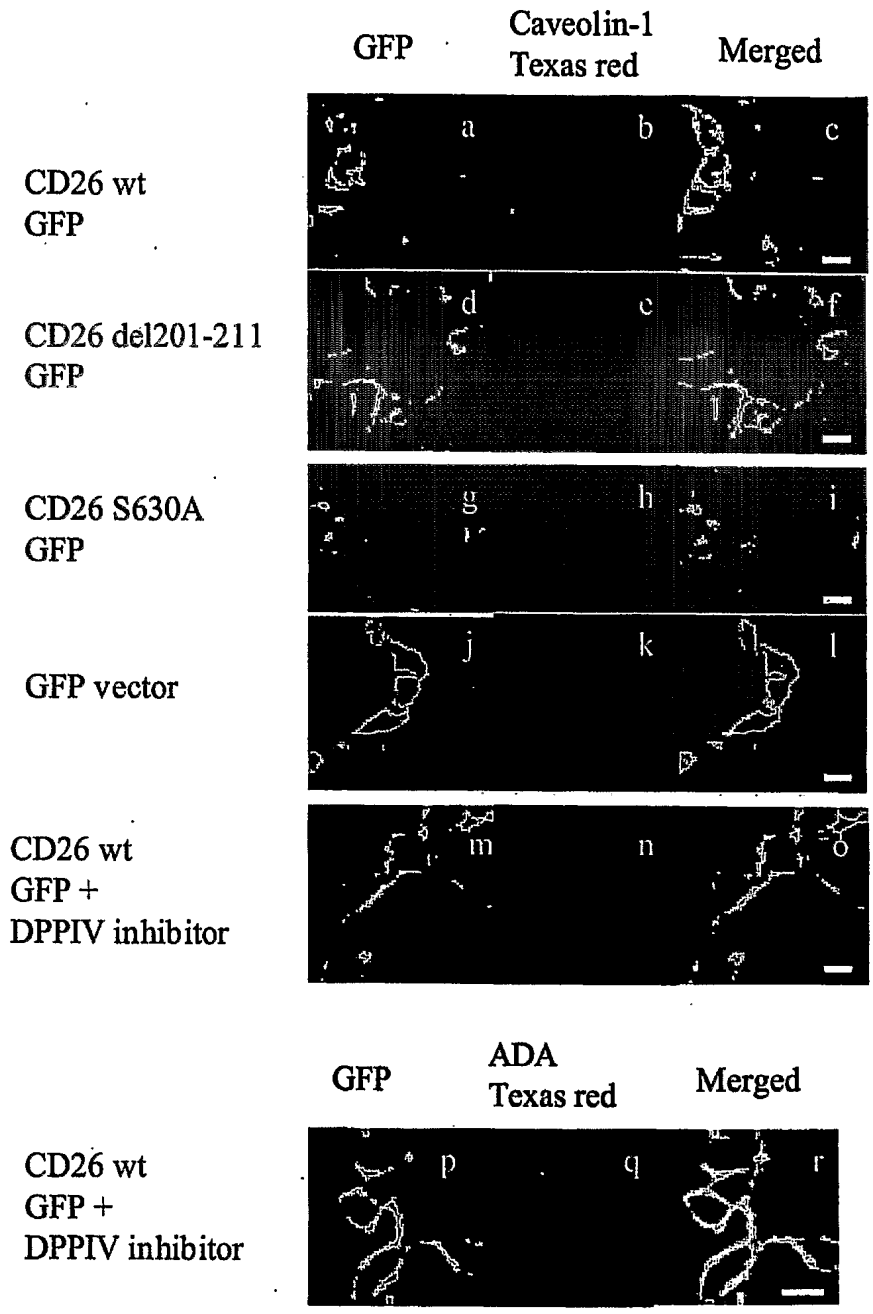

Copy provid..d b.. USPTO from the IFW Image Database on 01/11/2005

Figure 2

A

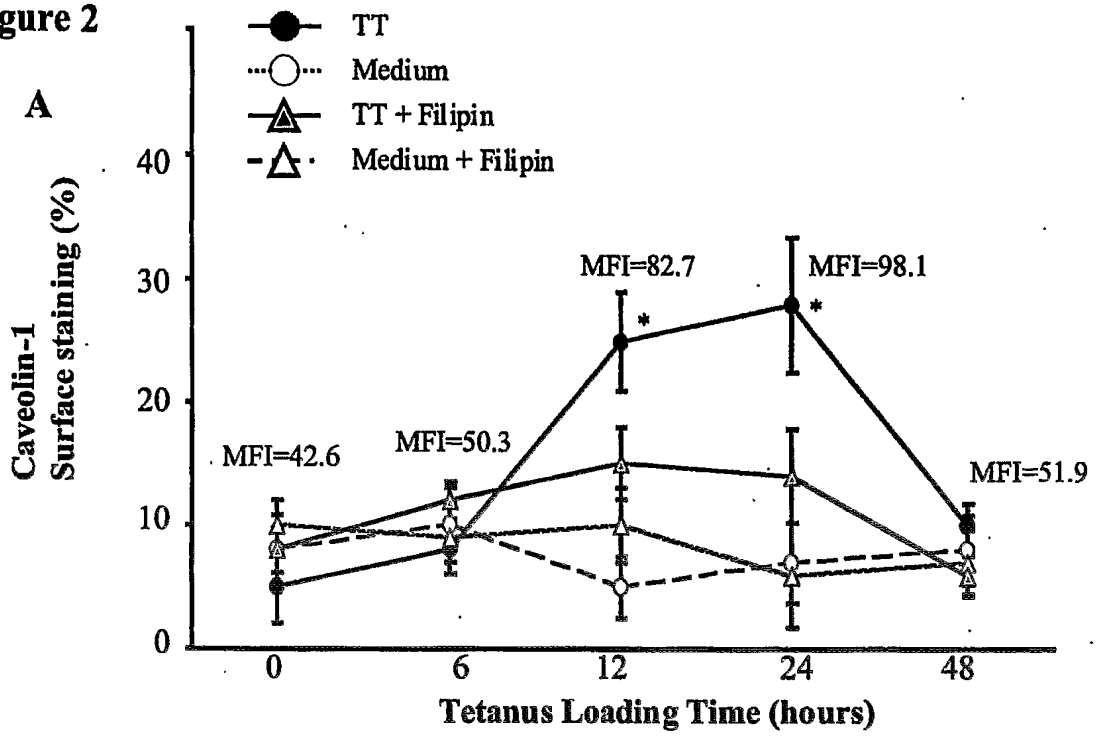

B

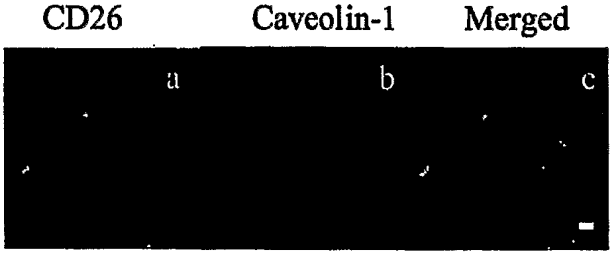

C

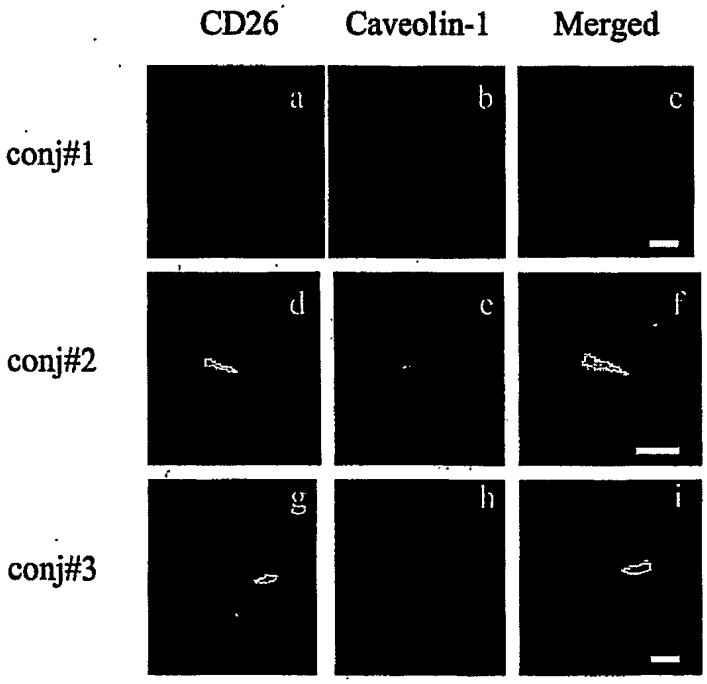

Co... d by USPTO f... th... IFW Image Database on 01/11/2005

Figure 2

D

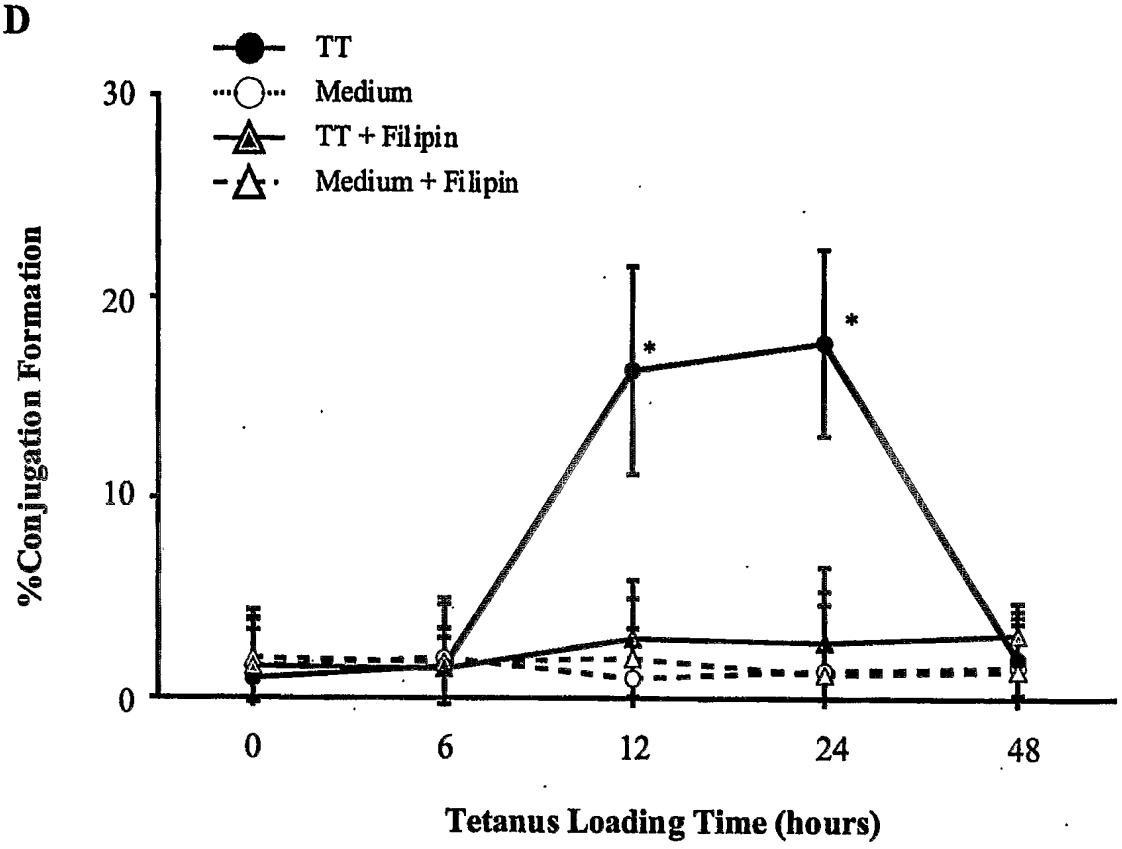

Copy provided by USPTO from the IFW Image Database on 01/11/2005

Figure 3

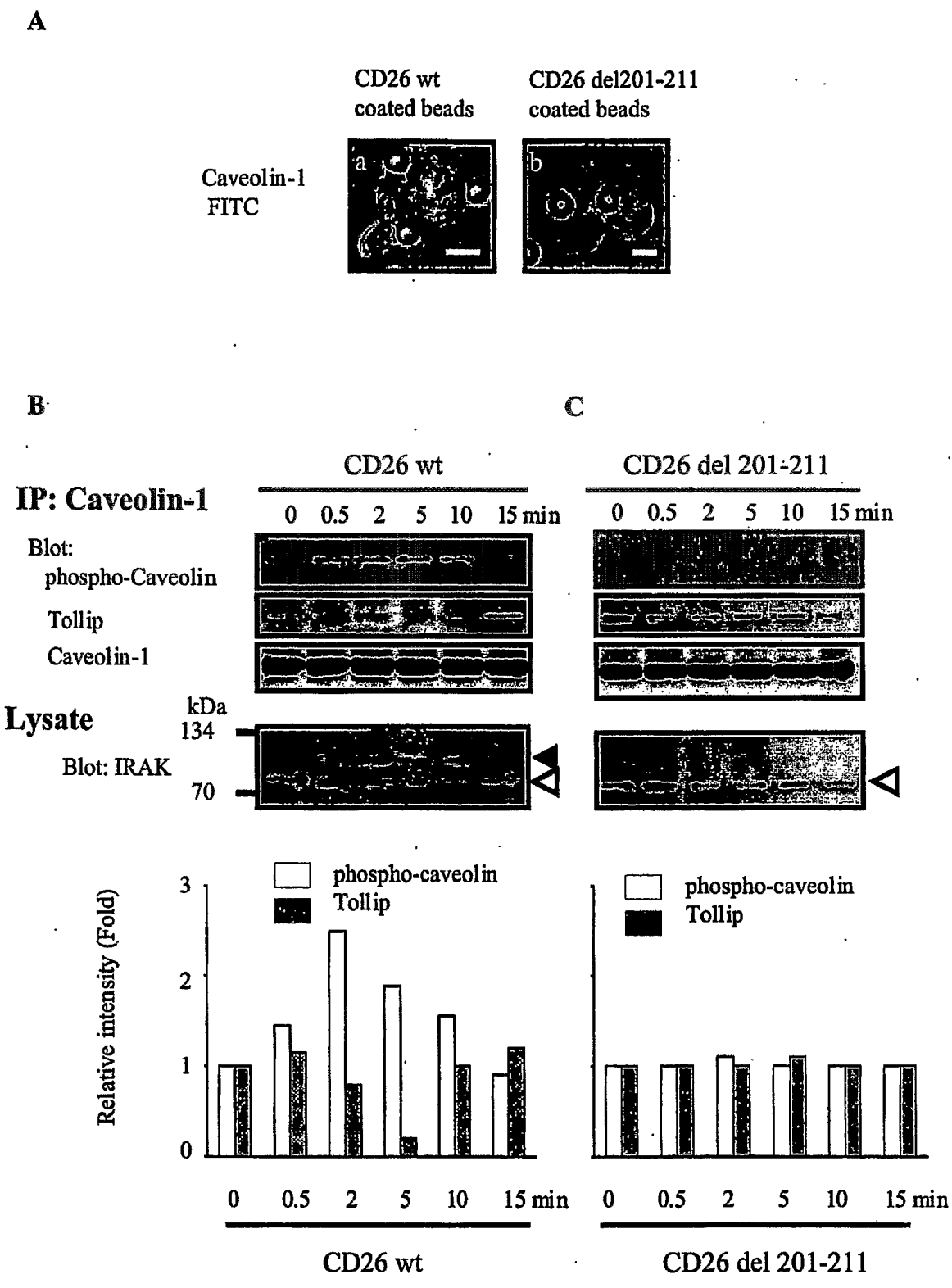

Copy provided by USPTO from the IFW Image Database on 01/11/2005

Figure 3

D

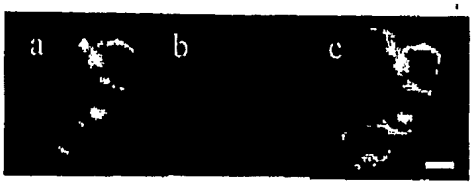

E

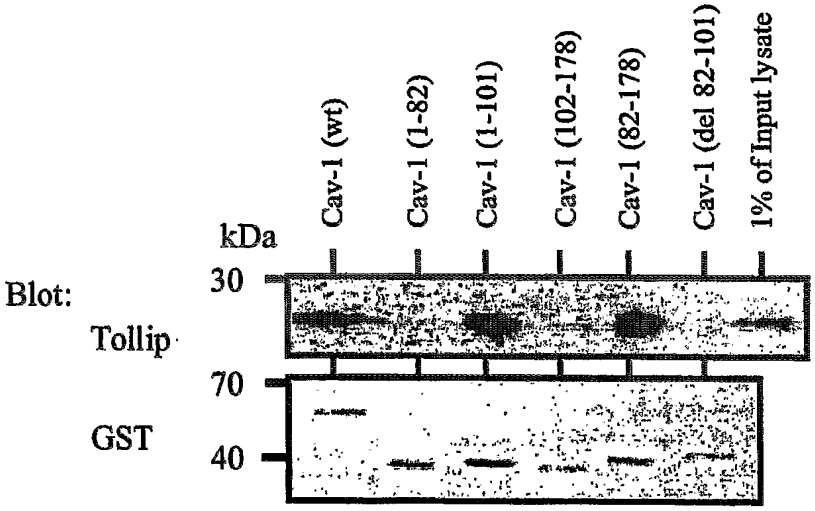

F

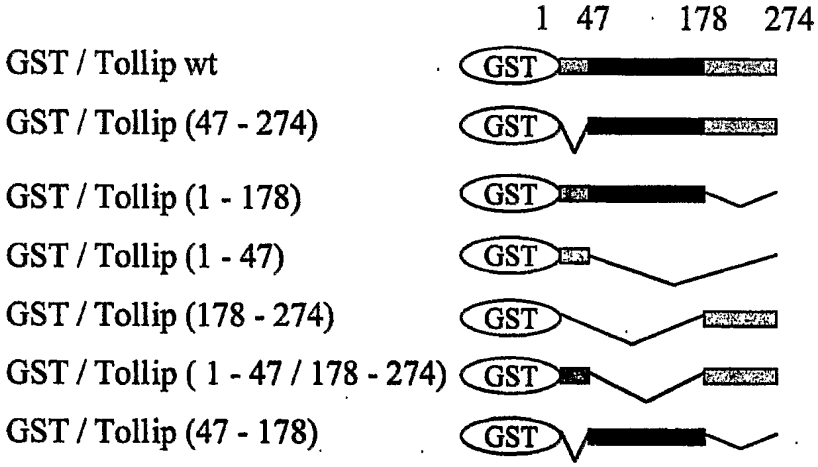

G

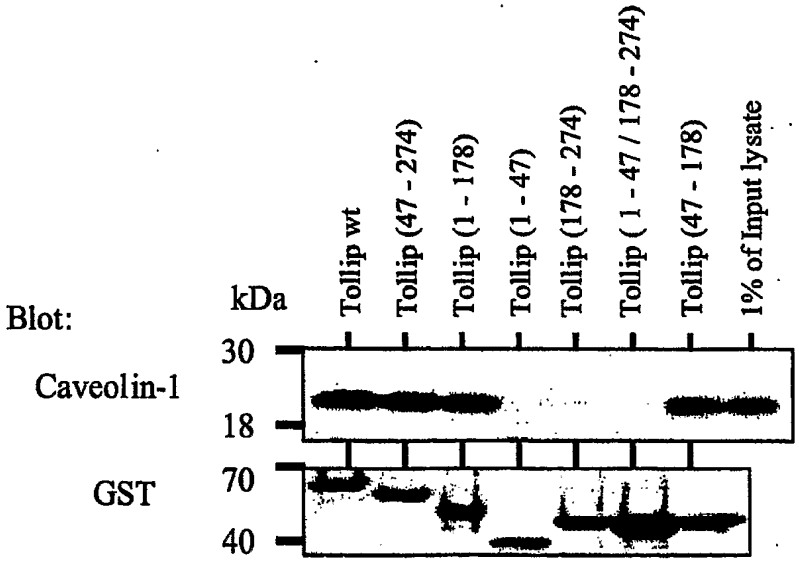

Generated by USPTO from the IFW Image Database on 01/11/2005

Figure 4

A

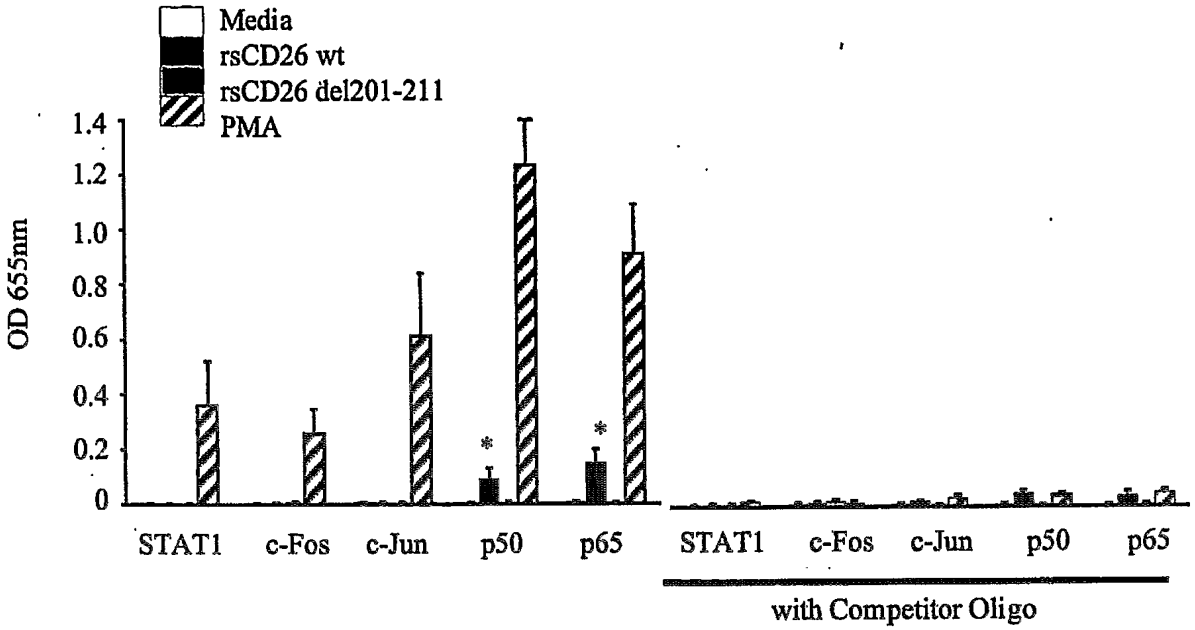

B

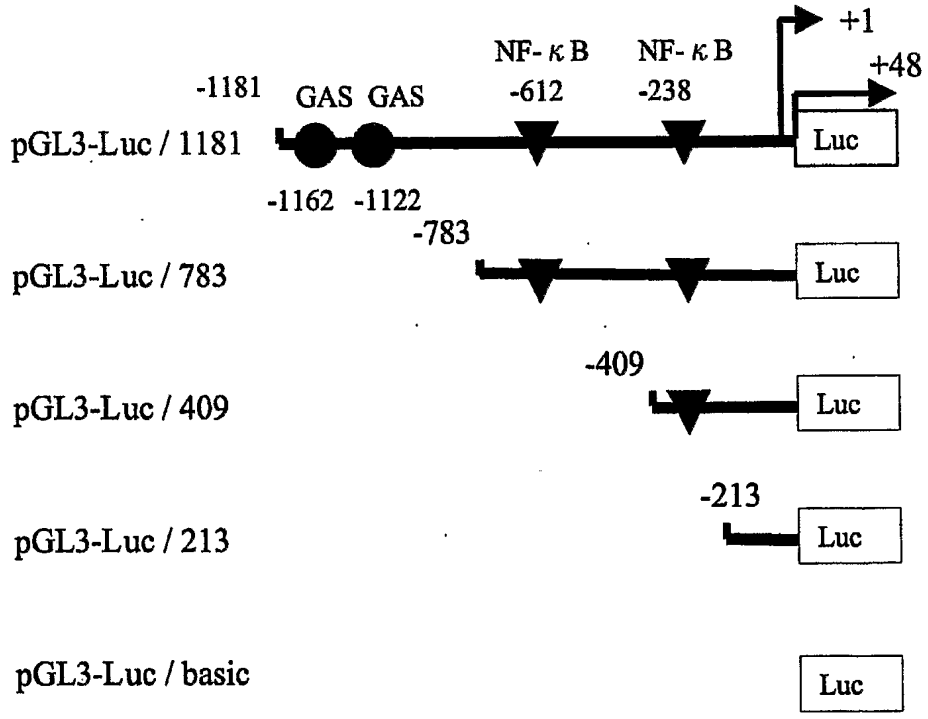

Generated by USPTO from the IFW Image Database on 01/11/2005

Figure 4

C

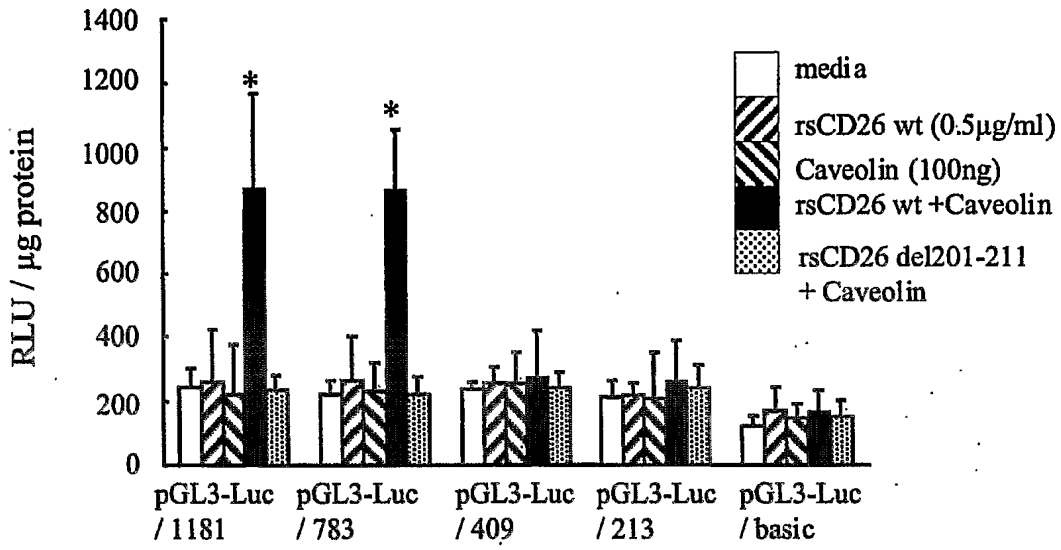

D

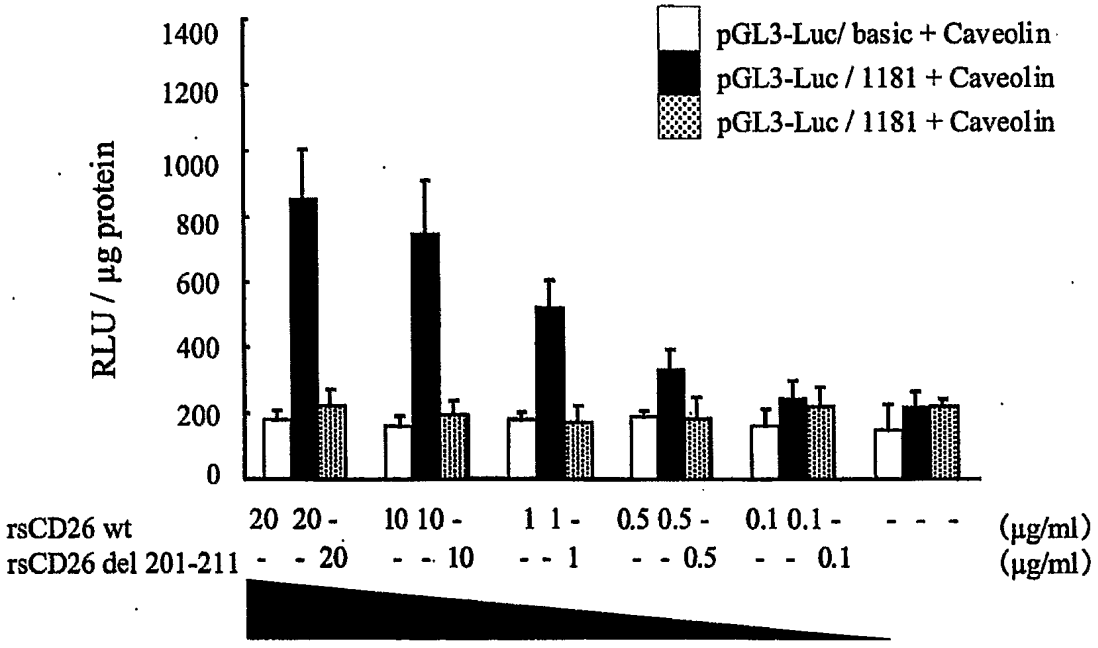

Copy provided by USPTO from the IFW Image Database on 01/11/2005

Figure 5

A

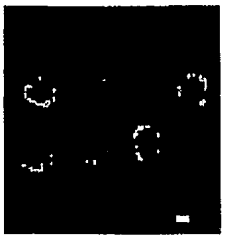

CD14 FITC +
Texas red siRNA

B

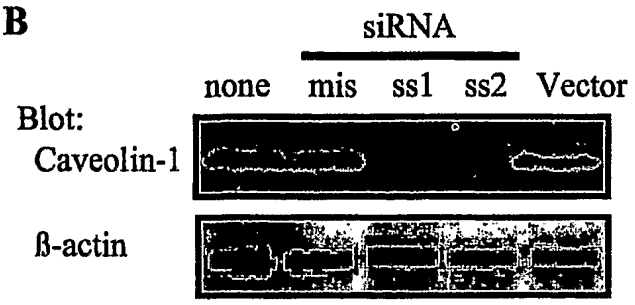

C

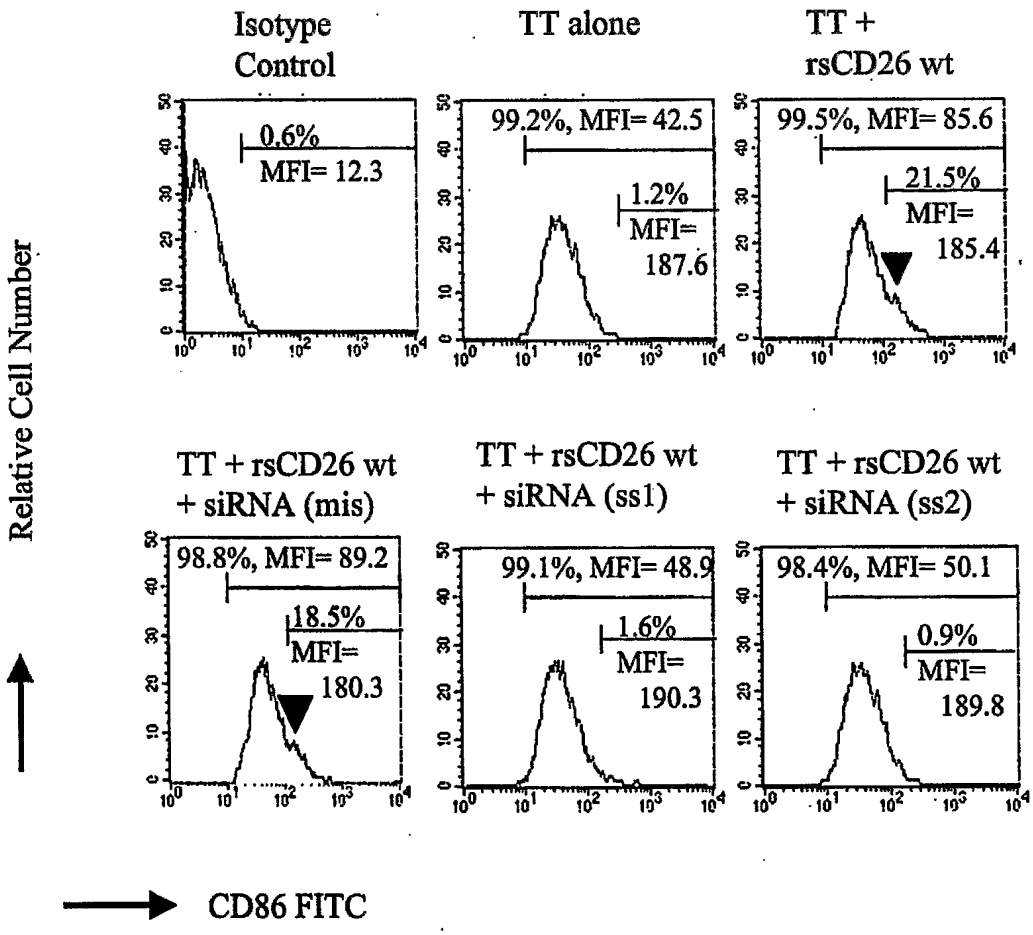

Copy provided by USPTO from the IFW Image Database on 01/11/2005

Figure 5

D

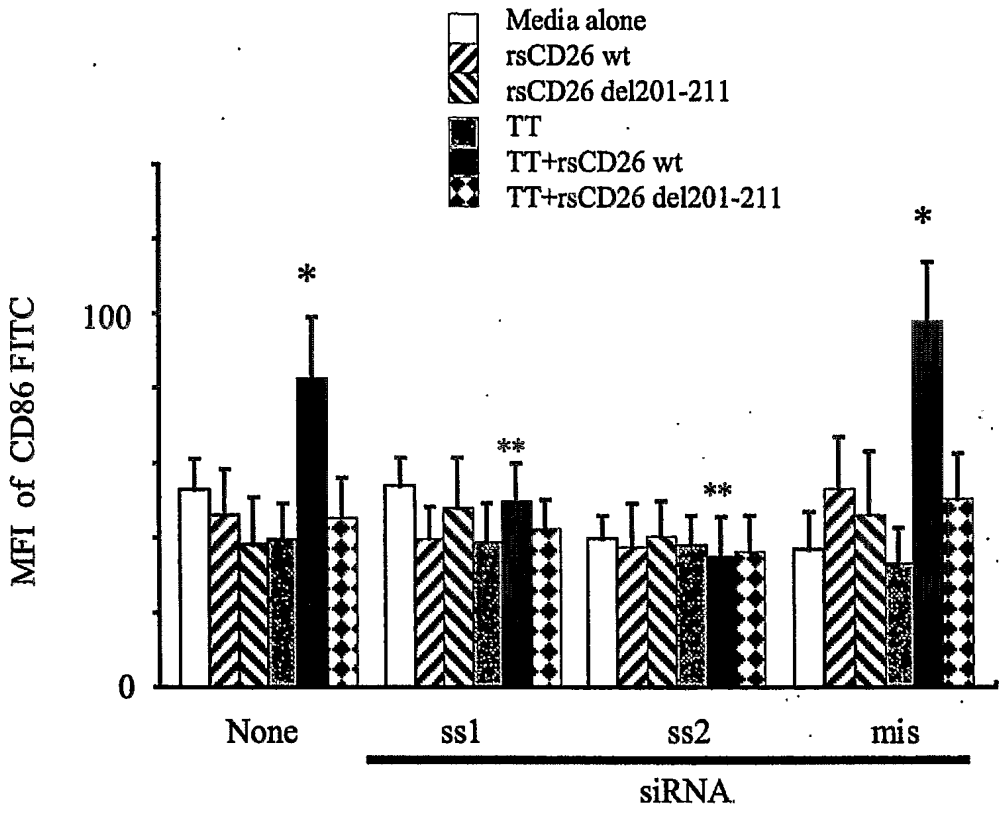
Media alone
rsCD26 wt
rsCD26 del201-211
TT
TT+rsCD26 wt
TT+rsCD26 del201-211
MFI of CD86 FITC
100
0
*
**
**
*
None
ss1
ss2
mis
siRNA

Figure 6

A

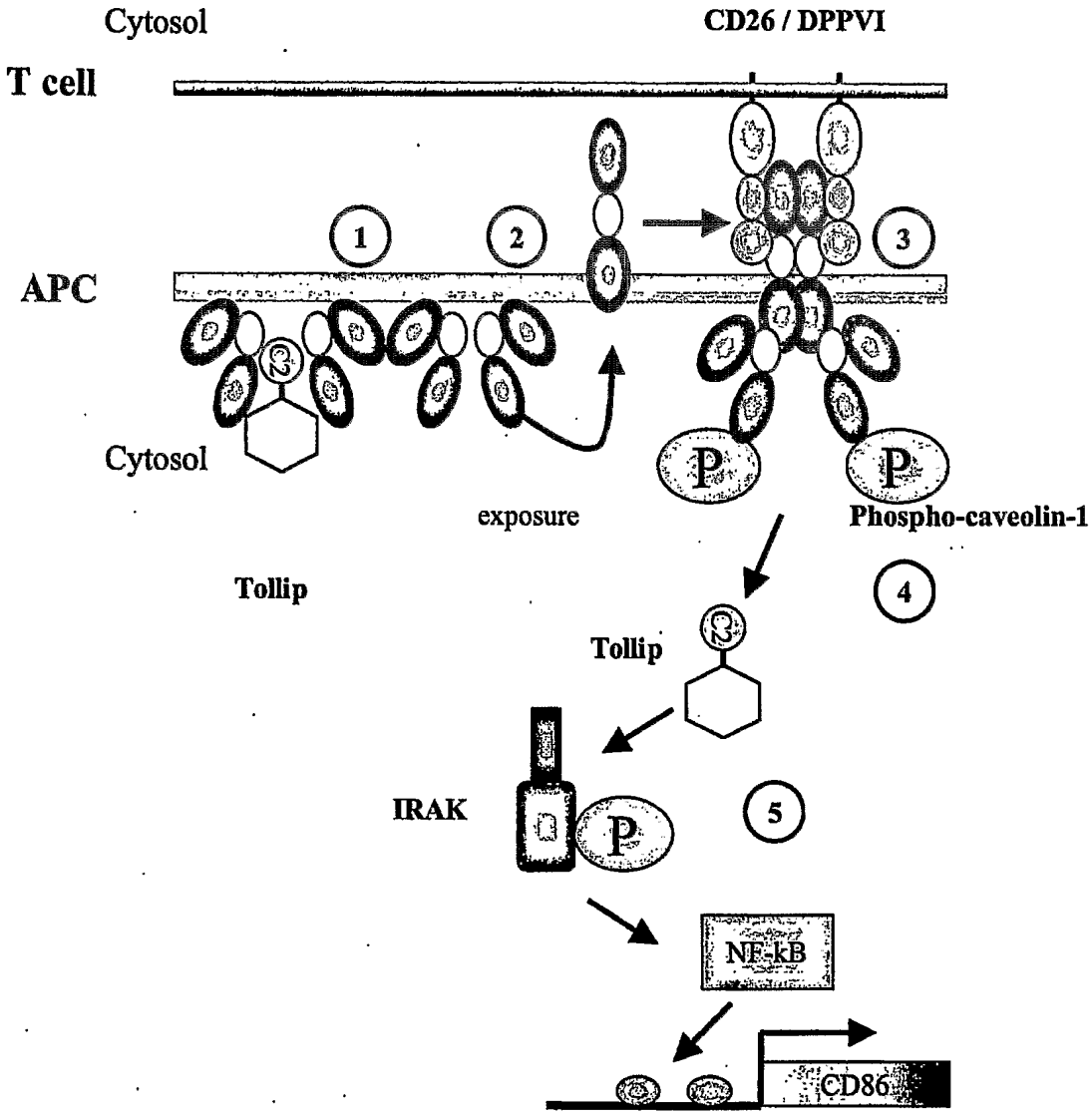

Copy provided by USPTO from the IFW Image Database on 01/11/2005

Figure 6

B

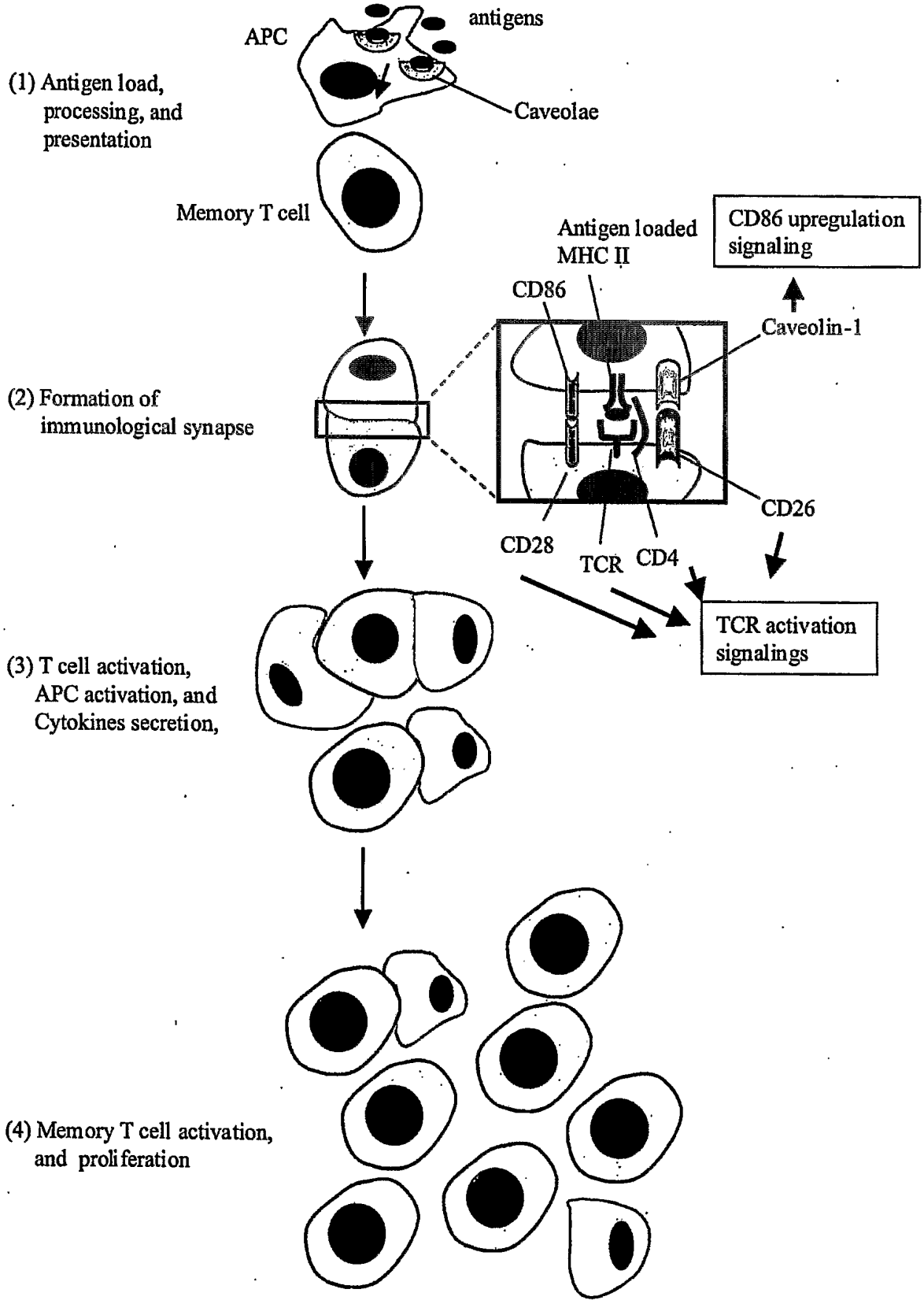

Copy provided by USPTO from the IFW Image Database on 01/11/2005

INVENTOR INFORMATION

Inventor One Given Name:: CHIKAO
Family Name:: MORIMOTO
City:: TOKYO
Country:: JAPAN
City of Residence:: TOKYO
Country of Residence:: JAPAN
Citizenship Country:: JAPAN
Inventor Two Given Name:: KEI
Family Name:: OHNUMA
City:: TOKYO
Country:: JAPAN
City of Residence:: TOKYO
Country of Residence:: JAPAN
Citizenship Country:: JAPAN

CORRESPONDENCE INFORMATION

Correspondence Customer Number:: 26111

APPLICATION INFORMATION

Title Line One:: METHODS FOR TREATING DISEASES IN NEED OF
Title Line Two:: REGULATION OF IMMUNE RESPONSE

Total Drawing Sheets:: 14
Formal Drawings?:: Yes
Application Type:: Provisional
Docket Number:: 2144.0150000
Secrecy Order in Parent Appl.?:: No

REPRESENTATIVE INFORMATION

Representative Customer Number:: 26111

Source:: PrintEFS Version 1.0.1

Copy provided by USPTO from the IFW Image Database on 01/11/2005